



Attribution–NonCommercial–NoDerivs 2.0 KOREA

You are free to :

- **Share** — copy and redistribute the material in any medium or format

Under the following terms :



Attribution — You must give [appropriate credit](#), provide a link to the license, and [indicate if changes were made](#). You may do so in any reasonable manner, but not in any way that suggests the licensor endorses you or your use.



NonCommercial — You may not use the material for [commercial purposes](#).



NoDerivs — If you [remix, transform, or build upon](#) the material, you may not distribute the modified material.

You do not have to comply with the license for elements of the material in the public domain or where your use is permitted by an applicable exception or limitation.

This is a human-readable summary of (and not a substitute for) the [license](#).

[Disclaimer](#) 

Thesis for the degree of doctor of philosophy

A Study on Vessel Motion Control

by

Anh-Minh Duc Tran

Department of Control and Mechanical Engineering

The Graduate School

Pukyong National University

February 2017

A Study on Vessel Motion Control

선박운동제어에 관한 연구

by

Anh-Minh Duc Tran

Advisor: Prof. Young-Bok Kim

**A thesis submitted in partial fulfillment of the requirements
for the degree of Doctor of Philosophy**

**In Department of Control and Mechanical Engineering,
The Graduate School,
Pukyong National University**

February 2017

A Study on Vessel Motion Control

A dissertation


by

Anh-Minh Duc Tran

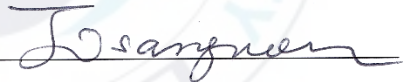
Approved by:



(Chairman) Prof. Jee-Youl Ryu



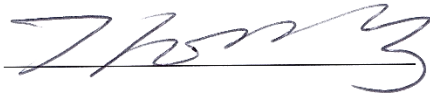
(Member) Prof. Ji-Seong Jang



(Member) Dr. Sang-Won Ji



(Member) Dr. Byung-Gak Kim



(Member) Prof. Young-Bok Kim

February 24th, 2017

Acknowledgement

First of all, I would like to express my sincere appreciation to Professor Young Bok Kim for his valuable advice and great guidance since my first days of my Ph.D. studying in Korea. His strong kindness and motivation encouraged and helped me to fulfill my research and complete this dissertation. I would like to wish my Professor and his family to have the long-lived health, safeness and happiness.

I would like to thank the members of my thesis committee: Prof. Jee-Youl Ryu, Prof. Ji-Seong Jang, Dr. Sang-Won Ji, and Dr. Byung-Gak Kim who have provided wonderful feedback on my work and great suggestions for better contribution of my dissertation.

I am particularly grateful to Dr. Hoang Duy Vo, Faculty of Electrical & Electronics Engineering and Ton Duc Thang University for essential assistances. I also thank to Dr. Van Phuoc Bui. Without their introduction and support I would not have the change to study in Korea. I am indebted to Prof. Thai Hoang Huynh at Ho Chi Minh City University of Technology who encouraged me all the time I studied.

I would like to thank all members of Marine Cybernetics Lab. For giving me a comfortable and active environment to achieve my work: Dac Chi Dang, Manh Son Tran, Van Trong Nguyen, Nhat Binh Le, Min Jae Jo, Seong Gi Ahn, Eun Ho Choi, Dong Hoon Lee, Joo Won Kim, Tae Wan Kim, Mi Roo Sin and all other Korean friends.

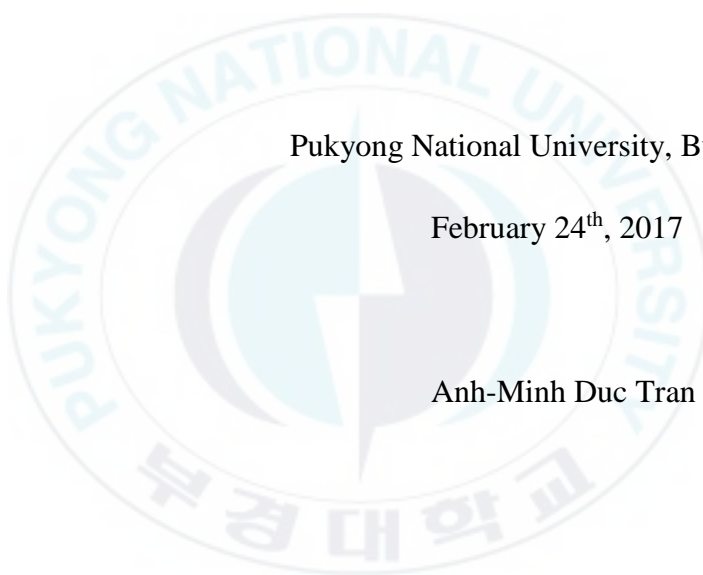
Thanks are also due to all members of PKNV, especially Huy Hung Nguyen, Trong Hai Nguyen, Viet Thang Tran, Hoang Phuoc Ho, Van Tu Duong, Duy Trinh Nguyen, Quang Tuyen Tran for their invaluable helps and vigorous supports.

Finally, I would like to thank my parents, my sisters, my brothers, my wife, and all my close relatives for their love, endless encouragements for me not only in the dissertation time but also in the whole of my life with their best wishes.

Pukyong National University, Busan, Korea

February 24th, 2017

Anh-Minh Duc Tran

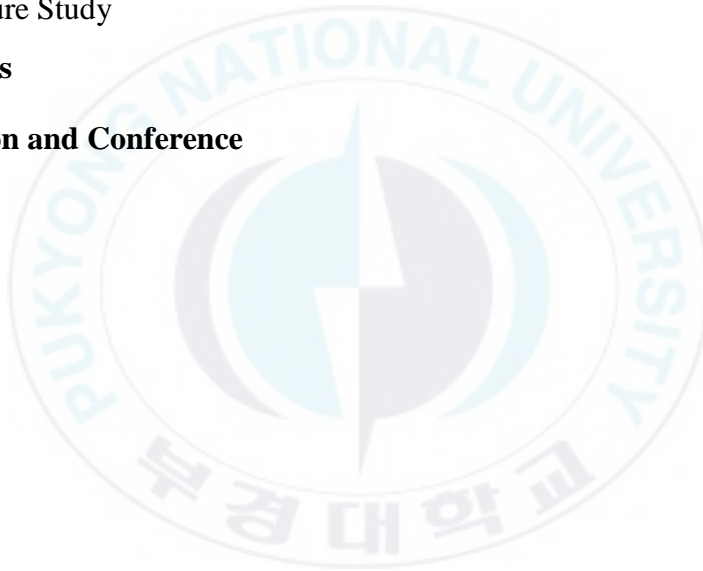


Contents

Contents	i
List of Figures	iv
List of Tables	vii
List of Abbreviations	viii
Nomenclatures	ix
Abstract	xv
Chapter 1. Introduction	1
1.1 Background and Motivation	1
1.1.1 Overview of Vessel Motion Control	1
1.1.1.1 Ship Berthing	1
1.1.1.2 Dynamic Positioning (DP)	2
1.1.1.3 Positioning Mooring (PM)	4
1.1.2 Overview of Rope Tension Control	5
1.1.2.1 Towing Rope Model	5
1.1.2.2 Mooring Rope Model	6
1.1.3 Motivation of Study	7
1.2 Objectives of Study	8
1.3 Organization of Thesis	8
Chapter 2. Control-Oriented Modeling of Towing Rope System	10
2.1 Introduction	10
2.2 System Modeling	12
2.2.1 Straight-line Towing Rope Model	12

2.2.2	Simplified Model for Towing Rope System	15
2.3	Controller Design and Simulation Results	19
2.3.1	Observer-based Servomechanism Design	19
2.3.2	Simulation Results	23
2.4	Summary	26
Chapter 3. System Identification and Control Design of Towing Rope		
	System	28
3.1	Introduction	28
3.2	Identification of Towing Rope System	28
3.2.1	System Configuration	28
3.2.2	Data Acquisition	31
3.2.3	Developed Plant Model	33
3.2.4	Uncertainty Analysis	34
3.3	Robust Control Design	36
3.3.1	Design Specifications	36
3.3.2	Open-loop and Closed-loop System Interconnections	39
3.3.3	μ -Synthesis	40
3.3.4	Order Reduction of μ -Controller	41
3.3.5	Analysis of Closed-loop System	44
3.4	Experimental Results	45
3.5	Summary	47
Chapter 4. Vessel Motion Control using Rope Tension Control Strategy		49
4.1	Introduction	49
4.2	Mathematical Modelling	49
4.2.1	Control Strategy	49
4.2.2	Vessel Motion	51

4.2.3 Multi-rope Mooring System Dynamics	53
4.3 Controller Design	55
4.4 Experiment	57
4.4.1 System Identification	57
4.4.2 Experimental Results	61
4.5 Summary	70
Chapter 5 Conclusion and Future Study	71
5.1 Conclusion	71
5.2 Future Study	73
References	74
Publication and Conference	83



List of Figures

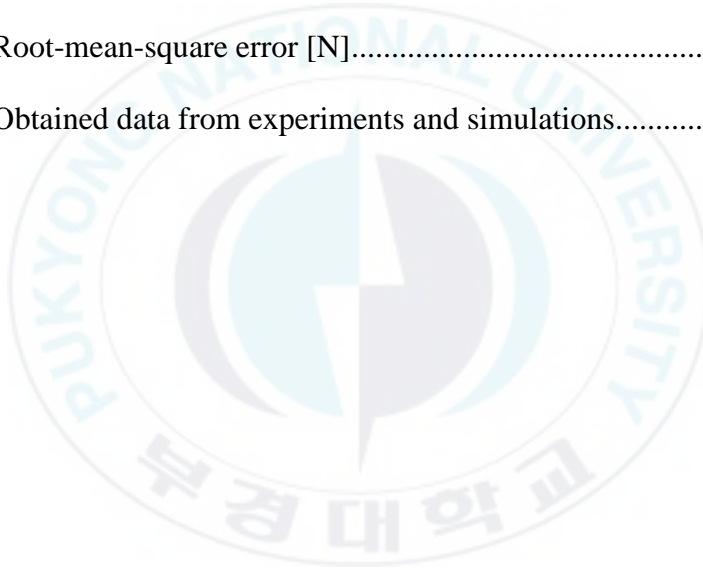
Fig. 1.1 Tugboat: Sea Tiger, Kamiya, Kasuga assisted the Yang Ming container ship berthing at C.M.I.T port	2
Fig. 1.2 A DP system with azimuth thrusters	3
Fig. 1.3 A PM system with 6 mooring lines	4
Fig. 2.1 Applications of cable-actuated system	10
Fig. 2.2 Straight line rope model	13
Fig. 2.3 Parameter variations of towing rope system.....	17
Fig. 2.4 Bode plot for the rope length of parameter-dependent towing rope system	18
Fig. 2.5 Impulse response of towing rope system (open-loop).....	19
Fig. 2.6 A reduced-order observer	22
Fig. 2.7 An observer-based servomechanism block diagram	23
Fig. 2.8 Simulation results of proposed reduced-order observer servomechanism control	25
Fig. 2.9 Comparison plots of controlled (proposed control method) and uncontrolled cases.....	26
Fig. 3.1 Schematic diagram of towing rope system.....	29
Fig. 3.2 Photo of towing rope system	29
Fig. 3.3 Photos of experimental apparatus.....	30
Fig. 3.4 Photo of data acquisition device USB NI-6229.....	31

Fig. 3.5 Chirp signal responses of towing rope system	32
Fig. 3.6 Uncertain frequency responses of the towing rope system	35
Fig. 3.7 Towing rope system uncertainty approximation	36
Fig. 3.8 Block diagram of the perturbed towing rope system.....	36
Fig. 3.9 Interconnection structure of the closed-loop system	37
Fig. 3.10 Open-loop interconnection structure of the towing rope system...	39
Fig. 3.11 Closed-loop interconnection structure of the towing rope system	39
Fig. 3.12 Frequency responses of the controller	41
Fig. 3.13 Relation between controller order and robust performance margin	42
Fig. 3.14 Bode plots of full and reduced-order controllers.....	43
Fig. 3.15 Robust stability for 2DOF controller.....	44
Fig. 3.16 Robust performance for 2DOF controller	45
Fig. 3.17 Transient responses of the robust and PID controller.....	46
Fig. 3.18 Reference tracking and error for rope length of 3m	47
Fig. 4.1 A vessel motion control strategy by using rope tension control.....	50
Fig. 4.2 Mooring rope configuration in vessel motion control	55
Fig. 4.3 Block diagram of control strategy	56
Fig. 4.4 Pulling vessel and measurement set-up for applied forces with load cells	59
Fig. 4.5 Obtained pulling force and vessel position.....	59

Fig. 4.6 Position and velocity data fitting results.....	60
Fig. 4.7 An overview of components for vessel motion control system.....	62
Fig. 4.8 Photos of linear motion actuator system.....	63
Fig. 4.9 Photos of tension measurement system	64
Fig. 4.10 Photo of ceiling CCD camera system.....	64
Fig. 4.11 Photo of real-time controller NI cRIO-9024 and modules	65
Fig. 4.12 Schematic diagram of experimental set-up	65
Fig. 4.13 Vessel motions in wave disturbance without control	66
Fig. 4.14 Station keeping experimental results in wave disturbance by using PI control	67
Fig. 4.15 Experimental results for a multi-step reference input in surge direction	68
Fig. 4.16 Experimental results for a multi-step reference input in sway direction	69
Fig. 5.1 Vessel berthing system assisted by damper and towing rope system	73

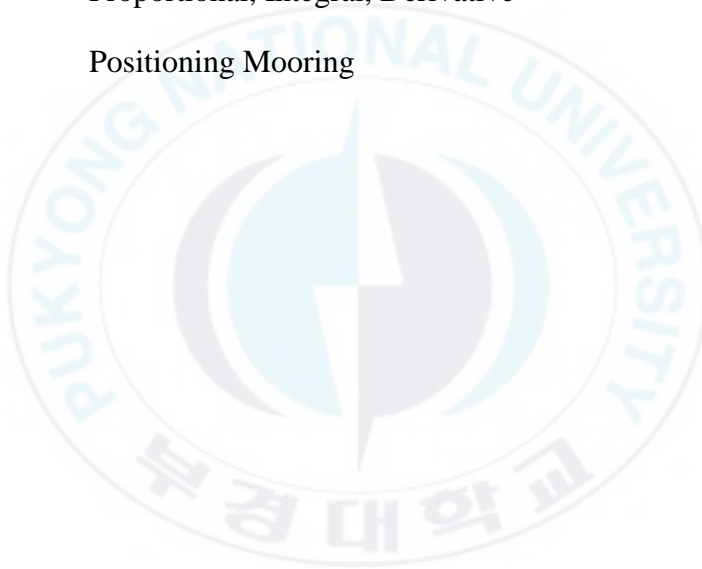
List of Tables

Table 2.1 Towing rope system parameters [64].....	15
Table 3.1 Estimated parameter values of towing rope model given in Eq. (3.1)	33
Table 3.2 Nominal parameter of towing rope transfer function	34
Table 3.3 Results of the μ -synthesis	41
Table 3.4 Root-mean-square error [N].....	47
Table 4.1 Obtained data from experiments and simulations.....	61



List of Abbreviations

2DOF	Two-Degree-of-Freedom
3DOF	Three-Degree-of-Freedom
DP	Dynamic Positioning
PI	Proportional, Integral
PID	Proportional, Integral, Derivative
PM	Positioning Mooring



Nomenclatures

Symbol	Description	Unit
a_1, a_2, a_3	Towing rope system model parameters	-
$\bar{a}_1, \bar{a}_2, \bar{a}_3$	Nominal value of towing rope system model parameters	-
A_r	Rope cross section	m ²
A	System matrix of towing rope system model	-
A_{11}, A_{12} A_{21}, A_{22}	Blocks of system matrix of towing rope system model	-
\hat{A}	Matrix of observer	-
b_0, b_1, b_2	Towing rope system model parameters	-
$\bar{b}_0, \bar{b}_1, \bar{b}_2$	Nominal value of towing rope system model parameters	-
b_c	Friction between cart and plane	N. s/m
b_w	Rotational viscous coefficient	N. m. s/rad
b_r	Damping constant of towing rope	N. s/m
B	Input vector of towing rope system model	-
B_1, B_2	Blocks of input vector of towing rope system model	-
B_r	Rope constant damping	Pa. s

\mathbf{C}	Output vector of towing rope system model	-
$\mathbf{C}_A(\mathbf{v}_r)$	Centripetal matrix	-
$\mathbf{C}_{RB}(\mathbf{v})$	Skew-symmetric Coriolis matrix	-
d	Input disturbance	-
$\mathbf{d}_{moor}(\mathbf{v})$	Additional damping	-
\mathbf{D}	Linear damping matrix	-
$\mathbf{D}(\mathbf{v}_r)$	Damping matrix	-
\mathbf{e}_b	Reduced estimation error	-
E_r	Rope modulus of elasticity	Pa
F_L	Lower linear fractional transformation	-
\mathbf{F}	Horizontal forces of mooring rope	-
\mathbf{F}_c	State feedback gain vector	-
$\mathbf{F}_{c1}, \mathbf{F}_{c2}$	Partitioned parts of state feedback gain vector	-
\mathbf{F}_i	Augmented feedback gain vector	-
$\bar{G}, \bar{G}(s)$	Nominal transfer function model of towing rope system	-
$\mathbf{G}(\boldsymbol{\eta})$	Generalized restoring vector	-
h_w	Width of winch	m
\mathbf{H}	Matrix of observer	-
J	Total inertia moment on winch	kg. m ²

J_w	Inertia moment of winch	kg. m ²
k_r	Spring constant of towing rope	N/m
K_D	Derivative parameter of PID controller	-
K_I	Integral parameter of PID controller	-
K_N	Filter coefficient of PID controller	-
K_P	Proportional parameter of PID controller	-
K_{PID}	PID controller	-
K_r	Feedforward controller	-
K_y	Feedback controller	-
K	Matrix of observer	-
K_P	Proportional gain matrix	-
K_I	Integral gain matrix	-
l_c	Current (stretched) length of rope	m
l_r	Length of towing rope	m
\bar{L}	Matrix of observer	-
m	Total mass on cart	kg
m_c	Mass of cart	kg
m_r	Mass of towing rope	kg
M	Low frequency system inertia matrix including the added mass	-

$P(s)$	Transfer function matrix	-
r	Step reference input	-
r_r	Radius of rope	m
r_w	Radius of winch	m
$R(\psi)$	Rotation matrix in heading direction	-
S	Sensitivity function	-
T	Complementary sensitivity function	-
T_w	Torque input to winch	N.m
$T(\alpha)$	Mooring rope configuration matrix	-
$T^+(\alpha)$	Pseudo-inverse of the mooring rope configuration matrix	-
u	System input	-
W_p	Performance weighting function	-
W_r	Ideal system model	-
W_u	Control weighting function	-
W_Δ	Uncertainty weighting function	-
x	Motion state vector of towing rope system	-
x_1	Motion state variable, position of right end of unstretched rope	m
x_2	Motion state variable, velocity of right end of unstretched rope	m/s

x_3	Motion state variable, position of right end of stretched rope	m
x_4	Motion state variable, velocity of right end of stretched rope	m/s
x_r	Position of right end of unstretched rope	m
x_c	Position of right end of stretched rope, position of cart	m
x_i	Integral of tracking error	-
$\mathbf{x}_a, \mathbf{x}_b$	Motion sub-states vector of towing rope system	-
$\hat{\mathbf{x}}$	State of observer	-
$\hat{\mathbf{x}}_a, \hat{\mathbf{x}}_b$	Sub-states of observer	-
y	System output	-
z_p, z_u	Output costs	-
\mathbf{z}	State of reduced order observer	-
α	Force direction of mooring ropes	-
δ_r	Rope mass per meter	kg/m
Δ	Unmodeled dynamics	-
Δ_p	Performance uncertainty block	-
Δ_F	Fictitious uncertainty	-
η	Vessel position and orientation vector in Earth-fixed frame	-

η_d	Desired positions and heading angle	-
λ_c	Control eigenvalues	-
λ_o	Observer eigenvalues	-
\mathbf{v}_r	Relative velocity vector considering the effect of current	-
$\boldsymbol{\tau}$	Input vector of forces in surge, sway and moment in yaw direction	-
$\boldsymbol{\tau}_c$	PI control law	-
$\boldsymbol{\tau}_{moor}$	Generalized mooring force	-
$\boldsymbol{\tau}_{thr}$	Thruster vector	-
$\boldsymbol{\tau}_{wave2}$	Second-order wave disturbance	-
$\boldsymbol{\tau}_{wind}$	Wind vector	-

A Study on Vessel Motion Control

Anh-Minh Duc Tran

**Department of Control and Mechanical Engineering,
The Graduate School, Pukyong National University**

Abstract

In the vessel motion control, ship berthing has been known as one of the most complicated and challenging procedures. The difficulties for berthing operation in the harbor could be outlined as the reduction in controllability at low speed, the effect of changes in hydrodynamic coefficients on ship handling, the large effect due to environmental disturbances, etc. Usually, tugboats should be used to assist it by pulling and pushing the vessel.

Another difficult task that vessel motion control had to face is the station keeping where constant or slowly-varying disturbances such as mean wind forces, mean currents and tidal currents need to be rejected. This is entirely handled by the positioning mooring (PM) system. Besides some vessels such as barges, disabled ships, semi-submersible rigs, drill ships, etc. could not move by themselves and need to be towed by tugboats.

In any case, rope is used as an indispensable facility, and rope tension control is the key point. In order to precisely and safely control the vessel's motion, the dynamic characteristics of the towing rope should be well examined.

This dissertation presents further study on modeling dynamics of towing rope system and applying rope tension control strategy on vessel motion control.

A control-oriented dynamic model of a towing rope system with variable length is established. In this simple model, a winch which is driven by a motor torque uses the towing rope to pull a cart. The rope is modeled as a straight and massless segment, and mass of rope is lumped partly to the cart and halfway to the winch. In addition, the changing spring constant and damping constant of towing rope are considered when the winch winds in. Finally, a reduced-order observer-based servomechanism controller is designed, and the overall system is verified by computer simulation.

Next, a rope tension control system is designed and implemented. A family of dynamic models of towing rope system are identified by changing the rope length. Among them, a representative model is selected, and the others are considered as uncertain models. Then, this work designs a μ -synthesis based on two-degree-of-freedom (2DOF) robust control system to cope with strong uncertainty and nonlinear property included in the real plant. An experimental comparison is conducted between the proposed control method and existing proportional–integral (PI) control method. The results indicate that the proposed method is more efficient and useful than the conventional one.

The problem of designing a PM system for a barge vessel is addressed. A model ship and four mooring systems used in this study are designed and created. The three-degree-of-freedom (3DOF) mathematical model of a system consisting of a barge ship and mooring systems is derived. Hydrodynamic coefficients of the low speed model for PM vessel are

identified by suitable experiments. A PI control scheme is implemented to achieve PM for the vessel by using rope tension control strategy. Real time control scheme integrating CompactRIO platform and LabVIEW program language is developed. The proposed strategy is finally tested on station keeping, and desired positions of the model vessel are obtained.



Chapter 1. Introduction

1.1 Background and Motivation

1.1.1 Overview of Vessel Motion Control

1.1.1.1 Ship Berthing

Maneuvering in harbor is recognized as being the most difficult procedure. Most of collisions and grounding of vessels appears during the maneuvering. The challenges of berthing vessels at harbor area include as follows:

- The controllability of main propeller reduces since low speed moving.
- The hydrodynamic coefficients change and influence on ship handling.
- The environmental disturbances such as wind, wave, current, etc. have adverse effects on vessel.

Various approaches have been proposed to solve these drawbacks. Preliminary works in this field primarily were from the 1990s by Japanese researchers. Kose and Jujuto [1] in 1987 was one of the first to develop a strategy for computer aided vessel berthing system. After, Kose and Hirao [2] introduced a procedure for estimating the abilities of tugboats operating with large ship and indicated that hydrodynamic forces induced by their interaction motions should be considered. A fully automatic berthing test was conducted in 1991 by Takai and Ohtsu [3]. In this research, the ship was maneuvered by using pitch propeller and tunnel thrusters. Shouji and Ohtsu [4-6] designed an optimal controller for ship berthing by using rudders, propellers and thrusters. Bui et al. [7] designed an optimal controller based on the observer for berthing ship by using bow and stern thrusters. In some cases, tugboats were used to assist ship maneuvering in the harbor as can be

seen in Fig. 1.1. With the purpose of ensuring safe berthing, Bui et al. [8] introduced a new method using autonomous tugboats.



Fig. 1.1 Tugboat: Sea Tiger, Kamiya, Kasuga assisted the Yang Ming container ship berthing at C.M.I.T port

Several studies have been performed on ship berthing using intelligent control theory. Takai and Yoshihisa [9] and Kasabeh et al. [10] used predictive fuzzy control method to build berthing system. Hasegawa and Kitera [11] and Hasegawa and Fukutomi [12] implemented neural network control to design an automatic berthing system. In [13] the authors introduced a multivariable neural network controller which is independent of the mathematical vessel model. A neural network controller was designed by Im and Hasegawa [14] to reduce the effects of disturbances.

1.1.1.2 Dynamic Positioning (DP)

The main purposes of a DP system are to maintain a specified position and heading as well as to maneuver a predefined track of marine vessel

unaffected by the disturbances acting upon it. The dynamically positioned vessel keeps its position entirely by means of the vessel's propulsion system as illustrated in Fig. 1.2.

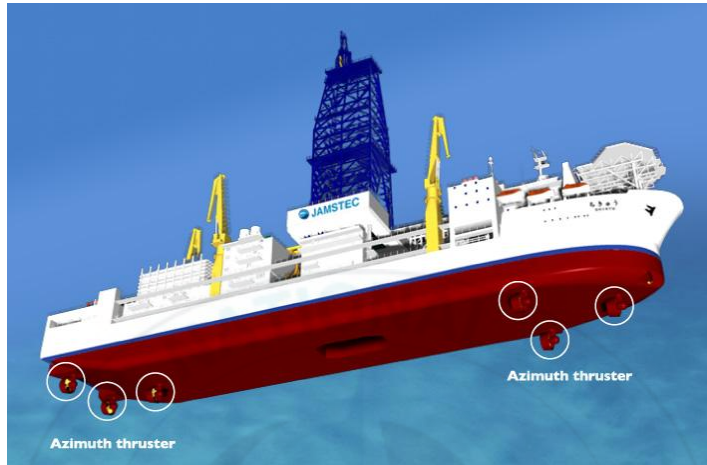


Fig. 1.2 A DP system with azimuth thrusters

There is a considerable amount of literature on DP system. Some preliminary works were carried out in the early 1960s, the first DP systems were presented to control horizontal-plane vessel motion by using single-input-single-output PID control strategy and low-pass and/or notch filter. More breakthrough techniques were introduced in the mid-1970s. Balchen et al. [15], Balchen et al. [16] and Saelid et al. [17] applied Kalman filter theory to avoid the time delay in estimation linear quadratic optimal in control design. Furthermore, the extended Kalman filtering techniques and stochastic optimal control theory were introduced in Grimbly et al. [18-19], Fung and Grimbly [20], Grimbly and Johnson [21] and Fossen [22]. In a major advance in 1999, Fossen and Strand [23] and Strand and Fossen [24] developed the nonlinear passive observer. This observer reduced significantly the observer gain matrix because the state space equations of the nonlinear observer were

depended on the nonlinear vessel's dynamics. Katebi and co-workers [25] designed a DP system with robust controller. Model-based nonlinear control design for DP system was proposed by Sorensen et al. [26]. Experiments on DP system with sliding mode control were carried out in 2010 by Tannuri et al. [27]. Sorensen [28] studied passive nonlinear observer based PID controller for operating up to extreme seas. More recent evidence [29-30] revealed a supervisory-switched controller for DP system for calm, moderate, high and extreme seas and for station keeping and maneuvering operations.

1.1.1.3 Positioning Mooring (PM)

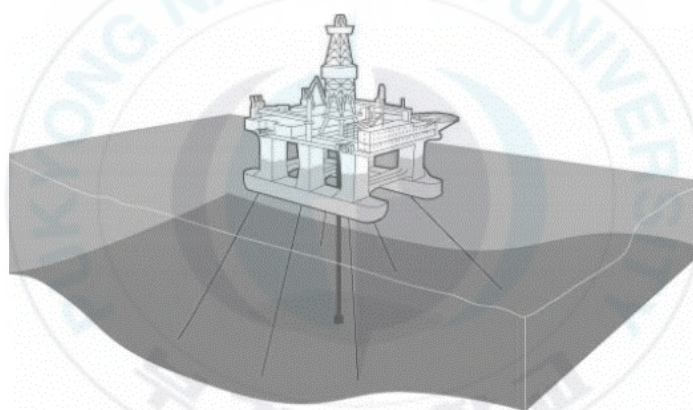


Fig. 1.3 A PM system with 6 mooring lines

However, compared to dynamic positioned vessels, moored vessel with thruster assistance is wide considered to be the most profitable and achievable solution. Due to the fact that the PM yields efficiently passive control at the intermediate water levels and the thrusters can produce active control to assist the mooring system when necessary in rough environmental conditions. The two main functions of PM are keeping the vessel in a desired position and heading and avoiding rope breakages by preserving the rope

tensions within a limited range. Fig. 1.3 shows a PM system of a semisubmersible drilling rig.

Many studies have been published on PM systems. In their seminal paper of 1998, Strand et al. [31] focused on the modelling and proposed a control strategy for thruster assisted PM system to meet the main function of maintain the vessel in a desired position. Afterward, Aamo and Fossen [32] studied about controlling the line tension in PM to guarantee the functions. Berntsen [33] proposed another control strategy by applying structural reliability measures for mooring ropes to keep the position of vessel. A set point chasing controller for thruster assisted PM vessel was proposed by Nguyen and Sorensen [34].

1.1.2 Overview of Rope Tension Control

With the above literature review, rope is recognized as being an indispensable facility and rope tension control is the key point. In order to precisely and safely control the vessel's motion, the dynamic characteristics of the towing rope should be well examined.

1.1.2.1 Towing Rope Model

Ship towing systems are widely engaged for towing un-propelled barges or disabled ships in berthing as well as maneuvering tasks. An improper towing system may introduce serious towing instability and lead to accidents, e.g. collisions. The stability of towed vessel will be effected by some factors such as the size of towed vessel, the environment disturbances and especially the towing system. Recently, the problems of towing operation, towing equipment, etc. have been considered.

In the literature, there are many theoretical approaches of modeling towing rope systems. In their cutting edge paper of 1950, Strandhagen et al. [35] used a single towline model to study course stability of the towed vessel, they also assumed constant towline tension. Kijima and Varyani [36] considered a rigid and straight towline when analyzing the characteristics of the course stability of a tow and two towed vessels under the wind pressure. Several studies, for example Bernitsas and Kekridis [37-38], Lee [39] and Jiang et al. [40] made use of a single elastic tow rope model. The authors considered the effects of length and material of the towrope on the stability. However, these researches did not present any controller to attenuate the effects of nonlinear elastic towline.

Another type of towline model was proposed by Nonaka et al. [41] and Yukawa et al. [42], in which the towline tension was calculated using catenary equations. Many attempts have been conducted by Fitriadhy and Yasukawa [43], Fitriadhy et al. [44] and Fitriadhy et al. [45] in order to establish a numerical model for course stability of a towed ship coupled to a tow ship through a towline. The towline motion was obtained by using 2D lumped mass method. Yoon and co-workers [46] divided the towing rope into multiple finite element which were connected by springs and dampers. Different scenarios were set up and simulated to confirm the proposed multiple finite element model. These towline models were well suited to analyze course stability, however, they were rather complex and difficult to obtain controller.

1.1.2.2 Mooring Rope Model

The dynamic characteristics of mooring ropes, chains and multi-component cables are increasingly becoming a vital factor in designing the

offshore mooring systems. Various approaches have been proposed to solve this issue.

In their seminal paper of 1997, Strand et al. [47] presented a line characteristics-base model for the mooring system which is obtained by solving the catenary equations. Next, a finite element model (FEM) of a mooring rope suspended in water was established in Aamo and Fossen [48]. Then, the authors [49] constructed a multi-cable mooring system model which was coupled to a floating vessel model. However, they did not introduce the controller for the system. In order to maintain the probability of the mooring system failure below an adequate level of safety in spite of environmental disturbances, Berntsen et al. [50] presented a controller by using a structural reliability measure for the mooring ropes. In [51], a switching control system for a PM system was proposed to integrate heading, damping, restoring and mean force controllers. The switching mechanism which automatically chose the needed controllers could increase the performance and safeness of the vessel under the varying environmental conditions. In [52], the authors designed a positioning controller for PM vessel to decrease the riser end angles. Many good results for control design of the mooring system were obtained, on the other hand, these studies mainly worked on the dynamics of the floating vessel, and neglected the dynamics of the mooring ropes.

1.1.3 Motivation of Study

Based on the above analyses, the motivation of this study is to develop a vessel motion control system by using rope tension control strategy. In this research, the dynamics of the towing rope system is considered and robust control algorithm is applied to cope with uncertainty and nonlinear property.

1.2 Objectives of Study

The objectives of this study are to

- Introduce a control-oriented dynamic model of a towing rope system.
- Build up the mathematical model for rope tension control system by doing experiment with swept sinusoidal signal and develop a robust control system which can cope with uncertainties.
- Build up the experimental model system to evaluate the efficiency of the rope tension approach.

1.3 Organization of Thesis

Chapter 1: Introduction

This chapter presents background and motivation of this dissertation. Objectives and researching methods are demonstrated. The organization of this thesis is given.

Chapter 2: Control-Oriented Dynamic Model of Towing Rope System

In this chapter, a control-oriented dynamic model of a system including a cart pulled by a variable length towing rope and a winch is presented. The modeling of the towing rope takes into account the varying spring constant and damping constant due to changing rope length. As well, the rope mass is lumped partly to the cart and partly to the winch. Since it is considered that the rope motion is difficult to measure, a reduced-order observer is introduced. In addition, a servomechanism controller is designed to precisely control the motion and obtain zero steady-state error in the towing rope system. The simulation results depict the effectiveness of the proposed

approach.

Chapter 3: System Identification and Control Design of Towing Rope System

A towing rope system is presented in this chapter. Since system parameters of the towing rope system depend on rope length, they are non-linear and difficult to obtain. A family of 3rd order transfer functions are used to represent the system. All parameters of the transfer functions are estimated based on the experimental data. A μ -synthesis based 2DOF robust control is designed to cope with strong uncertainty and nonlinear property included in the real plant. The effectiveness of the proposed rope tension controller is compared to that of PID controller through simulation and experimental results.

Chapter 4: Vessel Motion Control using Rope Tension Control Strategy

The rope tension control strategy for vessel motion control is proposed. The 3DOF mathematical model considering the motion of barge-type vessel in horizontal plane is proposed. The system inertia matrix and linear damping matrix of the vessel are obtained via identification process. A PI controller is designed to control motion of the vessel. The movement of the vessel is assisted by 4 mooring systems and tension of each mooring rope is determined by using control allocation technique. The effectiveness of the proposed strategy is evaluated through experiment.

Chapter 5: Conclusion and Future Study

The key research findings of this dissertation are summarized and some ideas for future work are presented.

Chapter 2. Control-Oriented Modeling of Towing Rope System

2.1 Introduction

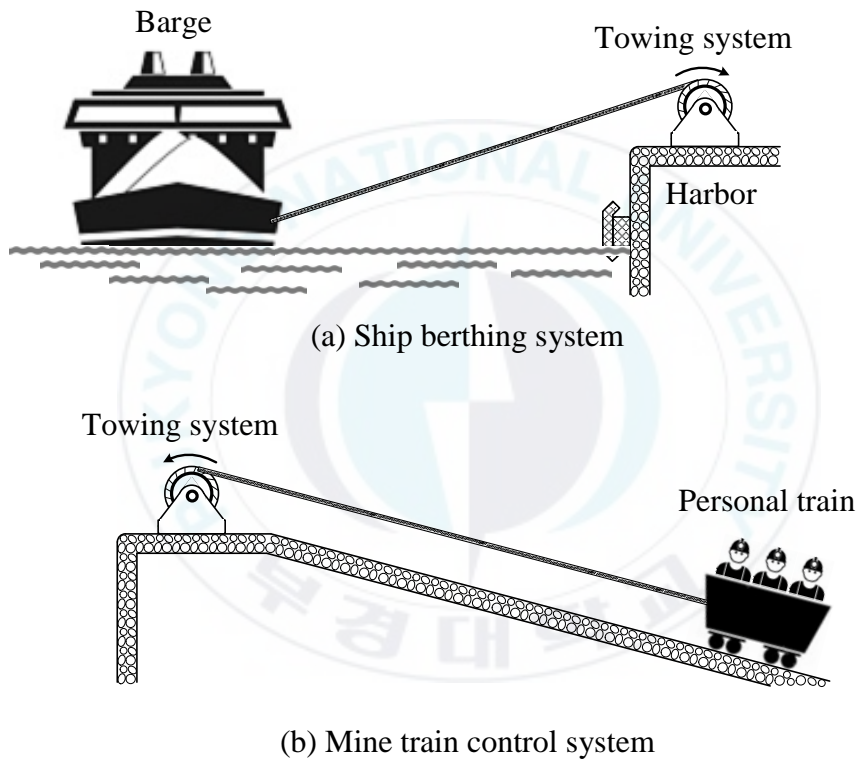


Fig. 2.1 Applications of cable-actuated system

Cables are attracting widespread interest due to their special characteristics, including high acceleration maneuvers and higher payload to weight ratios. Some of the applications that cables are presently being used for around the world include cable robots, elevators, cranes, mine train

transport systems, air-borne module-based wind energy units, berthing and mooring vessels, etc. [53-58]. Fig. 2.1 shows applications of cable-actuated system.

Unfortunately, it is quite difficult to control the loads and cables because the cables used in cable-actuated systems are often flexible. In the field of cable-driven robots, the cable is very light and stiff, and so cable dynamics can be neglected [59-60]. In spite of that, the mass and flexibility of the cables are significant and cannot be ignored in large-scale system. Thus, few studies have been published for modeling cable system by using lumped-mass method.

Milutinovic and Deur [61] introduced a multi-body approach to obtain dynamic model of varying tether length. In this paper, the rope model included a series of straight, massless and elastic segments with rope mass lumped to segment joints. The numbers of unwound segments were also changeable. This model accurately described the catenary form of the rope and analyzed motion of the rope. However, the model was rather complex and it would be difficult to design the controller.

According to Takeuchi and Liu [62], the elasticity of the long cable in the mine truck system created vibration which was troublesome and reduced the efficiency of the convey system. Thus, they constructed a simplified 3-mass spring model with parameter perturbations. The system was nonlinear and time-varying because mass and spring constant, and viscous friction depend on the position of the truck. So as to solve this problem, a time-invariant velocity controller was basically designed on the rationally scaled H_∞ control and simulation results showed good performance.

Further, Kang and Sul [63] suppressed the vibration for a lift car caused by the resonance of elastic ropes while the car was lifted. The rope mass was

neglected but the changes of spring constant and damping constant of rope were examined. Extended full-order observer based on acceleration feedback compensation was derived and verified through the simulations and experiments. Nevertheless, these researches just focused on velocity and/or acceleration control.

This chapter introduces a motion control system of a cart driven by a towing rope system. The important issue includes developing a dynamic model of a towing rope system in which rope parameters depend on changing in length of rope. In addition, it is considered that the rope motion is difficult to measure. Therefore, a reduced-order observer is designed to estimate the motion states of the towing rope system. Finally, the proposed method is proved by means of computer simulations.

2.2 System Modeling

2.2.1 Straight-line Towing Rope Model

A straight segment is given as a model of the towing rope. This is shown in Fig. 2.2 in which a cart is connected to a winch through virtual mechanical components of a spring and a damper. Here, the spring constant k_r and the damping constant b_r characterize the rope flexibility and are determined by change in length of towing rope l_r . According to Moon et al. [64], spring constant and damping constant can be calculated as Eqs. (2.1) and (2.2).

$$k_r = \frac{E_r A_r}{l_r} \quad (2.1)$$

$$b_r = \frac{B_r A_r}{l_r} \quad (2.2)$$

where E_r is the rope modulus of elasticity, A_r is the rope cross section, and B_r is the rope constant damping.

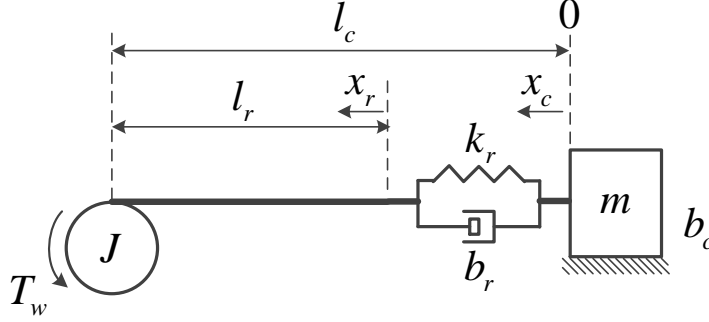


Fig. 2.2 Straight line rope model

The spread rope mass m_r is lumped to two ends of the rope, in order that half of the rope mass is appended to the winch inertia J_w and the other is added to the mass of the cart m_c . Thus, the total inertia moment on the winch and total mass on the cart are

$$m = m_c + \delta_r \frac{l_r}{2}, \quad (2.3)$$

$$J = J_w + \frac{l_r}{2} \delta_r \left(r_w^2 + \frac{3}{4} r_r^2 \right). \quad (2.4)$$

where δ_r is the rope mass per meter, and r_w and r_r are the radius of the winch and rope, respectively.

As illustrated in Fig. 2.2, l_r represents the variable length of the rope which is shortened when the winch winds in and l_c is the current (stretched) rope length which includes the natural (unstretched) rope length l_r introduced above and the rope stretch created by the flexible characteristics of the rope. Besides, x_r is the position of the right end of the unstretched rope and x_c is the position of the right end of the stretched rope which is also

the position of the cart. The dynamic system equation can be expressed as Eqs. (2.5) and (2.6).

$$\begin{cases} m\ddot{x}_c + b_c\dot{x}_c + k_r(x_c - x_r) + b_r(\dot{x}_c - \dot{x}_r) = 0 \\ J\frac{\ddot{x}_r}{r_w} + b_w\frac{\dot{x}_r}{r_w} + r_w k_r(x_r - x_c) + r_w b_r(\dot{x}_r - \dot{x}_c) = T_w \end{cases} \quad (2.5)$$

$$\Rightarrow \begin{cases} \ddot{x}_c = \frac{k_r}{m}x_r + \frac{b_r}{m}\dot{x}_r - \frac{k_r}{m}x_c - \frac{b_r + b_c}{m}\dot{x}_c \\ \ddot{x}_r = -\frac{r_w^2 k_r}{J}x_r - \frac{r_w^2 b_r + b_w}{J}\dot{x}_r + \frac{r_w^2 k_r}{J}x_c + \frac{r_w^2 b_r}{J}\dot{x}_c + \frac{r_w}{J}T_w \end{cases} \quad (2.6)$$

where T_w is the input torque of the winch motor, b_w is the rotational viscous coefficient caused by wire tension and friction force of the winch spindle and bearing, and b_c is the friction between the cart and the plane.

Finally, the state-space equation for motion of the cart driven by towing rope system can be derived as Eq. (2.7).

$$\begin{aligned} \mathbf{x} &= [x_1 \ x_2 \ x_3 \ x_4]^T = [x_r \ \dot{x}_r \ x_c \ \dot{x}_c]^T, \\ y &= x_1, \\ u &= T_w \end{aligned}$$

$$\begin{cases} \dot{\mathbf{x}} = \mathbf{A}\mathbf{x} + \mathbf{B}u \\ y = \mathbf{C}\mathbf{x} \end{cases} \quad (2.7)$$

with

$$\mathbf{A} = \begin{bmatrix} 0 & 1 & 0 & 0 \\ -\frac{r_w^2 k_r}{J} & -\frac{r_w^2 b_r + b_w}{J} & \frac{r_w^2 k_r}{J} & \frac{r_w^2 b_r}{J} \\ 0 & 0 & 0 & 1 \\ \frac{k_r}{m} & \frac{b_r}{m} & -\frac{k_r}{m} & -\frac{b_r + b_c}{m} \end{bmatrix},$$

$$\mathbf{B} = \begin{bmatrix} 0 & \frac{r_w}{J} & 0 & 0 \end{bmatrix}^T,$$

$$\mathbf{C} = [1 \quad 0 \quad 0 \quad 0]$$

2.2.2 Simplified Model for Towing Rope System

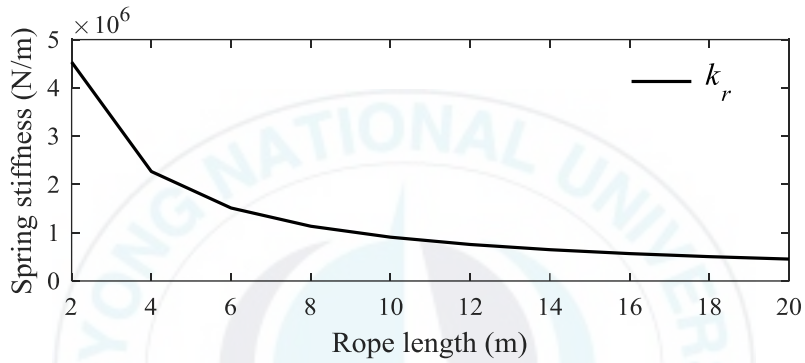
Table 2.1 Towing rope system parameters [64]

Item	Parameter	Value	Unit
Winch			
Radius	r_w	0.085	m
Width	h_w	0.22	m
Density steel	δ_w	8000	kg/m ³
Inertia moment	J_w	0.095	kg.m ²
Viscous coefficient	b_w	50	N.m.s/rad
Wire rope			
Cross section area	A_r	47x10 ⁻⁶	m ²
Elasticity modulus	E_r	193x10 ⁹	Pa
Constant of damping	B_r	5.2x10 ⁹	Pa.s
Total rope length	l	20	m
Radius	r_r	0.0039	m
Mass per meter	δ_r	0.2388	kg/m
Cart			
Mass	m_c	300	kg
Viscous friction	b_c	3000	N.s/m

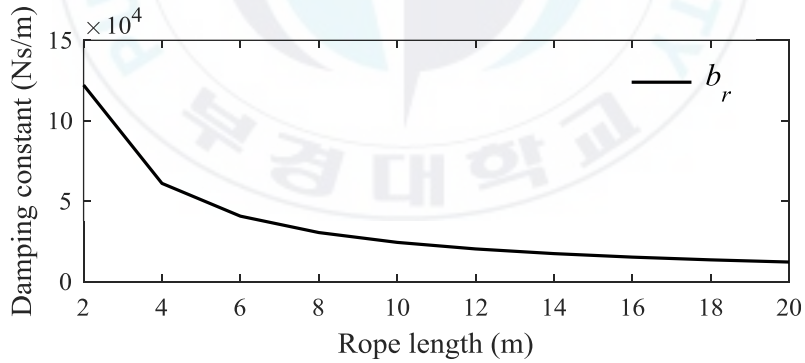
As the winch winds in to maneuver the cart, the length of rope varies the values of the total inertia moment of the winch, the total mass on the cart, the

damping constant and spring constant on the towing rope. These parameters are analyzed with assumption that the length of rope varies from 2m to 20m, and using the simulation parameters in S. M. Moon et al. [64] summarized in Table 2.1.

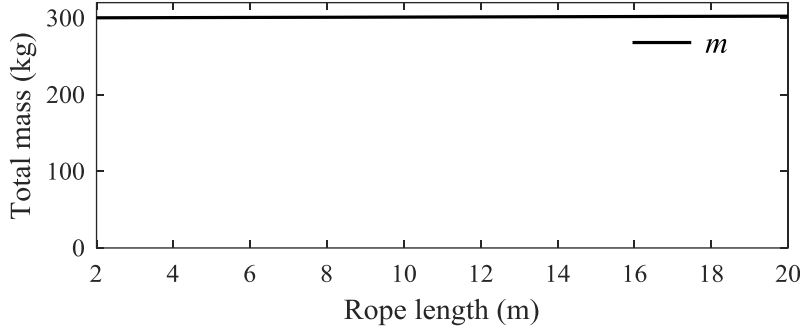
Fig. 2.3 shows parameter variations of towing rope system as listed in Table 2.1.



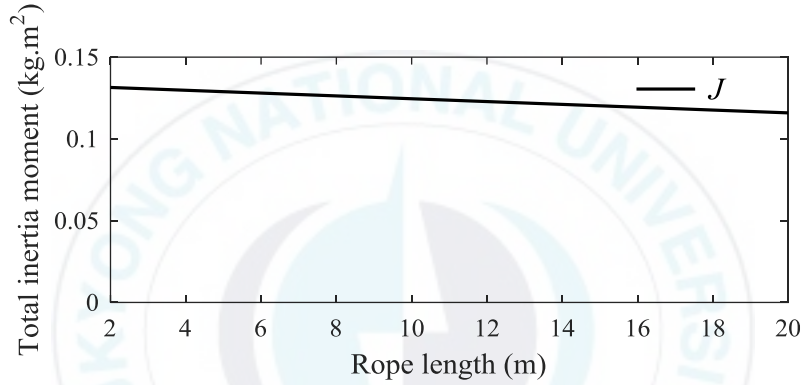
(a) Rope length vs. spring stiffness



(b) Rope length vs. damping constant



(c) Rope length vs. total mass



(d) Rope length vs. total inertia moment

Fig. 2.3 Parameter variations of towing rope system

As can be seen in Fig. 2.3, the spring constant and the damping constant of the rope change a lot when the rope length changes. However, the total inertia moment on the winch and the total mass on the cart vary a little. Thus, lumped mass of rope on the winch and the cart can be eliminated, and the state space equation of the system can be simplified, and it is expressed as Eq. (2.8).

$$\begin{cases} \dot{\mathbf{x}} = \mathbf{A}\mathbf{x} + \mathbf{B}u \\ \mathbf{y} = \mathbf{C}\mathbf{x} \end{cases} \quad (2.8)$$

with

$$\begin{aligned}
\mathbf{A} &= \begin{bmatrix} 0 & 1 & 0 & 0 \\ -\frac{r_w^2 k_r}{J_w} & -\frac{r_w^2 b_r + b_w}{J_w} & \frac{r_w^2 k_r}{J_w} & \frac{r_w^2 b_r}{J_w} \\ 0 & 0 & 0 & 1 \\ \frac{k_r}{m_c} & \frac{b_r}{m_c} & -\frac{k_r}{m_c} & -\frac{b_r + b_c}{m_c} \end{bmatrix}, \\
\mathbf{B} &= \begin{bmatrix} 0 & \frac{r_w}{J_w} & 0 & 0 \end{bmatrix}^T, \\
\mathbf{C} &= [1 \quad 0 \quad 0 \quad 0]
\end{aligned}$$

Fig. 2.4 shows the frequency response of the towing rope system with various lengths.

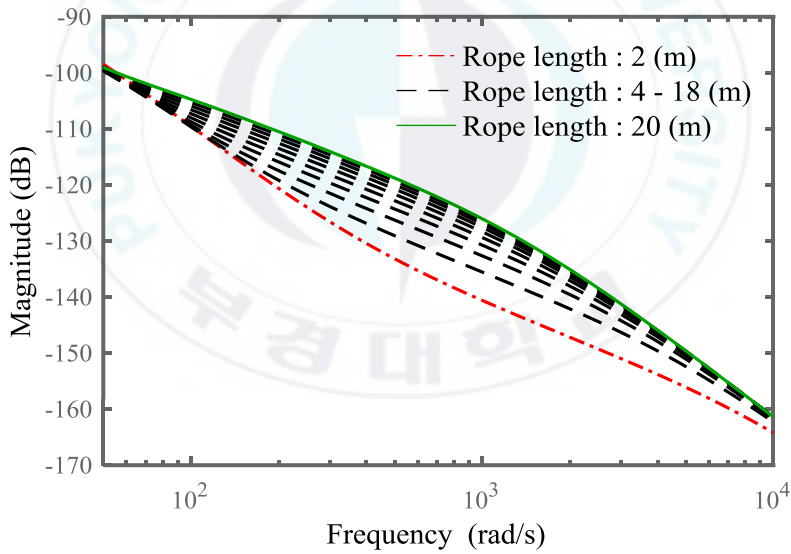


Fig. 2.4 Bode plot for the rope length of parameter-dependent towing rope system

In addition, an impulse response of open-loop system is implemented to verify the reduced model of towing rope system. As shown in Fig. 2.5, after

applying input torque, the winch rotates and winds in rope, and the unstretched rope length is shortened. However, the length of the stretched rope differs with the length of the unstretched rope. This mismatch appears due to the flexible characteristics of the towing rope.

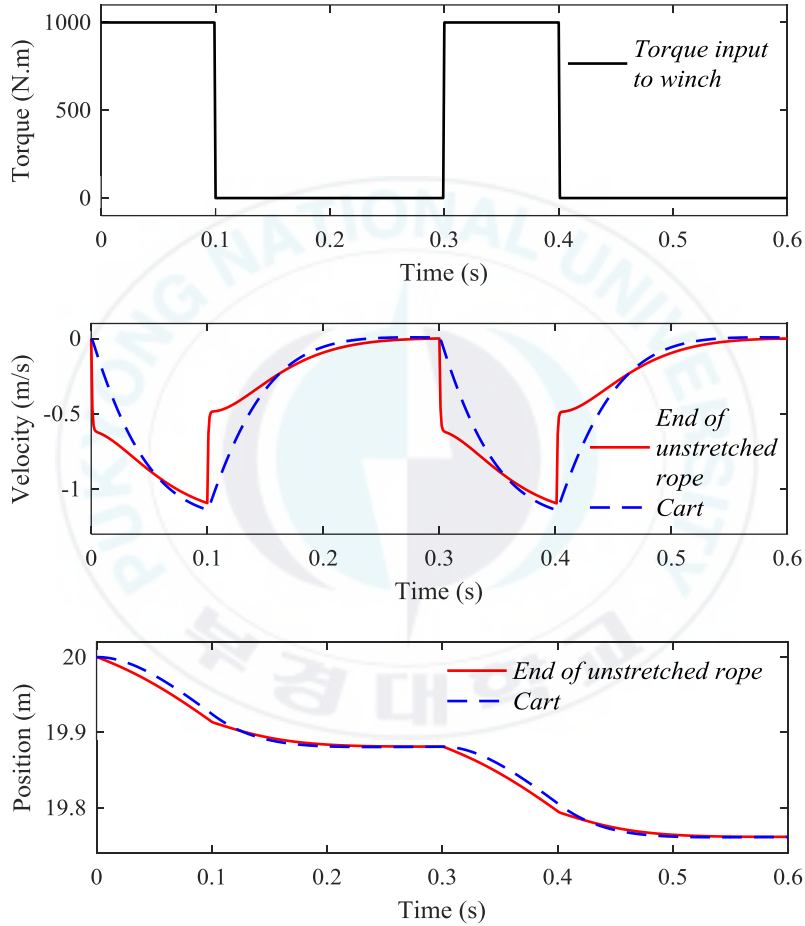


Fig. 2.5 Impulse response of towing rope system (open-loop)

2.3 Controller Design and Simulation Results

2.3.1 Observer-based Servomechanism Design

In order to precisely control the motion and obtain zero steady-state error in the towing rope system, a servomechanism design methodology [65] is applied. Furthermore, a reduced-order observer [66] is designed to estimate the states because it is uneasily considered to measure the rope motion states.

The open-loop towing rope system described in Eq. (2.8) can be partitioned as Eq. (2.9).

$$\begin{cases} \dot{\mathbf{x}} = \begin{bmatrix} \mathbf{A}_{11} & \mathbf{A}_{12} \\ \mathbf{A}_{21} & \mathbf{A}_{22} \end{bmatrix} \mathbf{x} + \begin{bmatrix} \mathbf{B}_1 \\ \mathbf{B}_2 \end{bmatrix} u, \\ \mathbf{y} = \mathbf{C}\mathbf{x} \end{cases} \quad (2.9)$$

with

$$\begin{aligned} \mathbf{A}_{11} &= 0, \\ \mathbf{A}_{12} &= [1 \quad 0 \quad 0], \\ \mathbf{A}_{21} &= \begin{bmatrix} -\frac{r_w^2 k_r}{J_w} & 0 & \frac{k_r}{m_c} \end{bmatrix}^T, \\ \mathbf{A}_{22} &= \begin{bmatrix} -\frac{r_w^2 b_r + b_w}{J_w} & \frac{r_w^2 k_r}{J_w} & \frac{r_w^2 b_r}{J_w} \\ 0 & 0 & 1 \\ \frac{b_r}{m_c} & -\frac{k_r}{m_c} & -\frac{b_r + b_c}{m_c} \end{bmatrix}, \\ \mathbf{B}_1 &= 0, \\ \mathbf{B}_2 &= \begin{bmatrix} \frac{r_w}{J_w} & 0 & 0 \end{bmatrix}^T, \\ \mathbf{C} &= [1 \quad 0 \quad 0 \quad 0] \end{aligned}$$

The state vector is separated into two sub-states to make the description of the reduced-order observer simplifier of Eq. (2.10).

$$\mathbf{x} = [\mathbf{x}_a \quad \mathbf{x}_b^T] \quad (2.10)$$

such that

$$\mathbf{x}_a = x_1 = y = \mathbf{C}\mathbf{x} \quad (2.11)$$

is the measurement vector, and

$$\mathbf{x}_b = [x_2 \quad x_3 \quad x_4]^T \quad (2.12)$$

contains the components of the state vector that cannot be directly measured.

Regarding \mathbf{x}_a and \mathbf{x}_b , the plant dynamics can be written as Eq. (2.13).

$$\begin{aligned} \dot{\mathbf{x}}_a &= \mathbf{A}_{11}\mathbf{x}_a + \mathbf{A}_{12}\mathbf{x}_b + \mathbf{B}_1u, \\ \dot{\mathbf{x}}_b &= \mathbf{A}_{21}\mathbf{x}_a + \mathbf{A}_{22}\mathbf{x}_b + \mathbf{B}_2u \end{aligned} \quad (2.13)$$

There is no need to design observer for \mathbf{x}_a because \mathbf{x}_a is directly measured by Eq. (2.14).

$$\hat{\mathbf{x}}_a = \mathbf{x}_a = x_1 = y \quad (2.14)$$

We define the reduced-order observer for \mathbf{x}_b of the remaining sub-state.

$$\hat{\mathbf{x}}_b = \mathbf{K}y + \mathbf{z} \quad (2.15)$$

where \mathbf{z} is the state of a system of order 3.

$$\dot{\mathbf{z}} = \hat{\mathbf{A}}\hat{\mathbf{x}}_b + \bar{\mathbf{L}}y + \mathbf{H}u \quad (2.16)$$

Fig. 2.6 shows the block diagram of the reduced-order observer. The matrices $\hat{\mathbf{A}}, \bar{\mathbf{L}}, \mathbf{H}$ and \mathbf{K} are chosen to ensure that the error in the estimation of the state converges to zero independent of x, y and u .

$$\begin{aligned}\hat{\mathbf{A}} &= \mathbf{A}_{22} - \mathbf{K}\mathbf{A}_{12}, \\ \bar{\mathbf{L}} &= \mathbf{A}_{21} - \mathbf{K}\mathbf{A}_{11}, \\ \mathbf{H} &= \mathbf{B}_2 - \mathbf{K}\mathbf{B}_1\end{aligned}\tag{2.17}$$

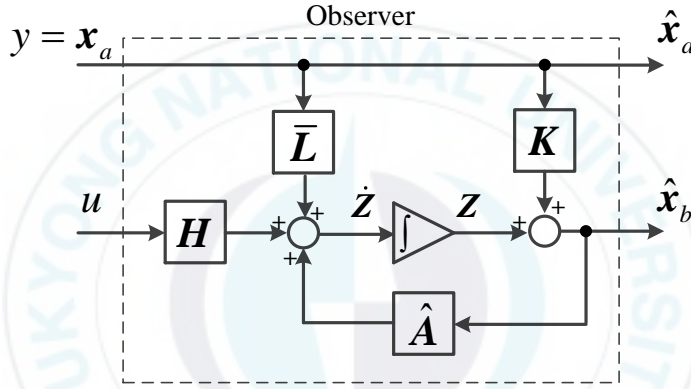


Fig. 2.6 A reduced-order observer

The servomechanism reduced-order observer-based compensator is the form of Eq. (2.18).

$$\begin{aligned}\dot{\mathbf{x}} &= (\mathbf{A} - \mathbf{B}\mathbf{F}_c)\mathbf{x} + \mathbf{B}\mathbf{F}_i\mathbf{x}_i + \mathbf{B}\mathbf{F}_{c2}\mathbf{e}_b, \\ \dot{\mathbf{x}}_i &= r - y, \\ \dot{\mathbf{e}}_b &= (\mathbf{A}_{22} - \mathbf{K}\mathbf{A}_{12})\mathbf{e}_b\end{aligned}\tag{2.18}$$

where r is the reference signal, $\mathbf{e}_b = \mathbf{x}_b - \hat{\mathbf{x}}_b$ is the error vector in estimation of \mathbf{x}_b , $\mathbf{F}_c = [\mathbf{F}_{c1} \quad \mathbf{F}_{c2}]$ is the state feedback gain vector, and \mathbf{F}_i is the augmented feedback gain.

These equations can be repackaged as Eq. (2.19).

$$\begin{bmatrix} \dot{x} \\ \dot{x}_i \\ \dot{e}_b \end{bmatrix} = \begin{bmatrix} A - BF_c & BF_i & BF_{c2} \\ -C & 0 & 0 \\ 0 & 0 & A_{22} - KA_{12} \end{bmatrix} \begin{bmatrix} x \\ x_i \\ e_b \end{bmatrix} + \begin{bmatrix} 0 \\ 1 \\ 0 \end{bmatrix} r \quad (2.19)$$

The observer-based servomechanism block diagram is shown in Fig. 2.7.

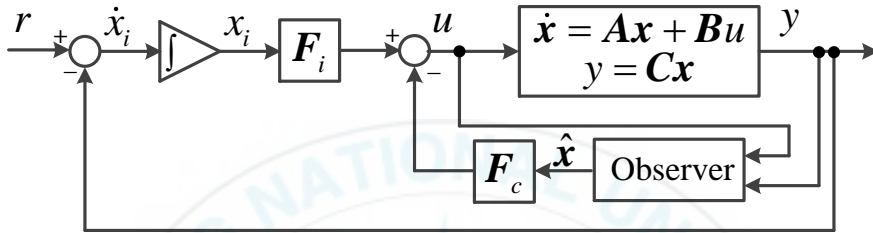


Fig. 2.7 An observer-based servomechanism block diagram

2.3.2 Simulation Results

In this dissertation, pole placement technique is used to determine the feedback gain matrix and the estimator gain matrix.

Control eigenvalues are chosen as Eq. (2.20).

$$\lambda_c = [-53.7 \quad -59.1 \quad -64.4 \quad -69.8 \quad -75.2] \quad (2.20)$$

, and these values yield the augmented state feedback gain vector of Eq. (2.21).

$$\begin{aligned} & [F_c \quad -F_i] \\ & = [-389380 \quad -11086 \quad 393590 \quad 10584 \quad -82399] \end{aligned} \quad (2.21)$$

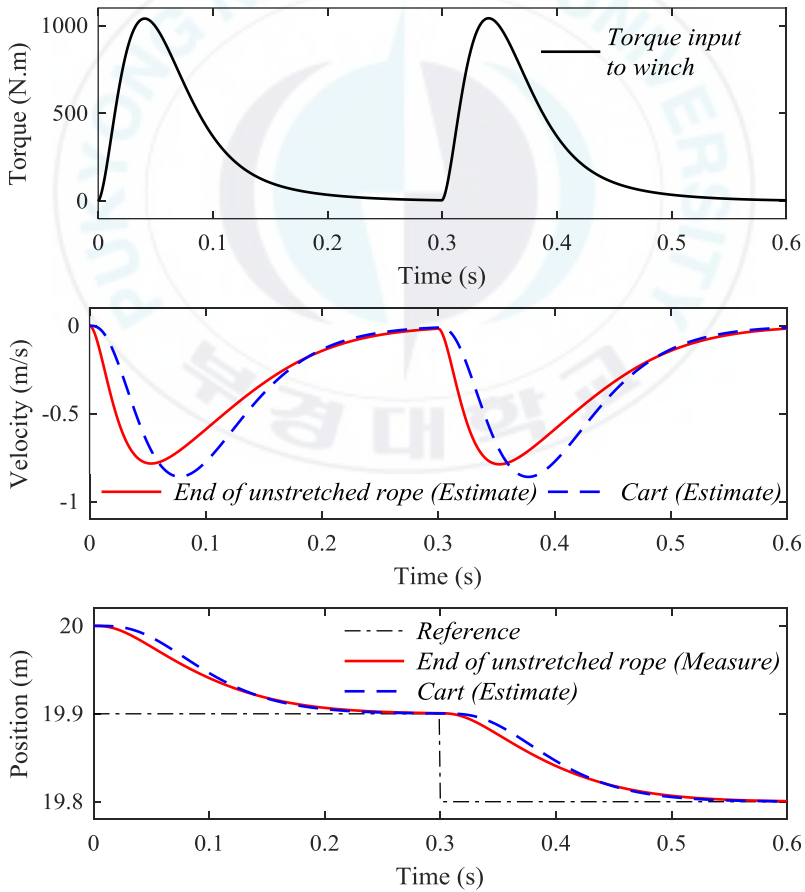
Observer eigenvalues are also chosen as Eq. (2.22).

$$\lambda_o = [-805 \quad -1611 \quad -2416] \quad (2.22)$$

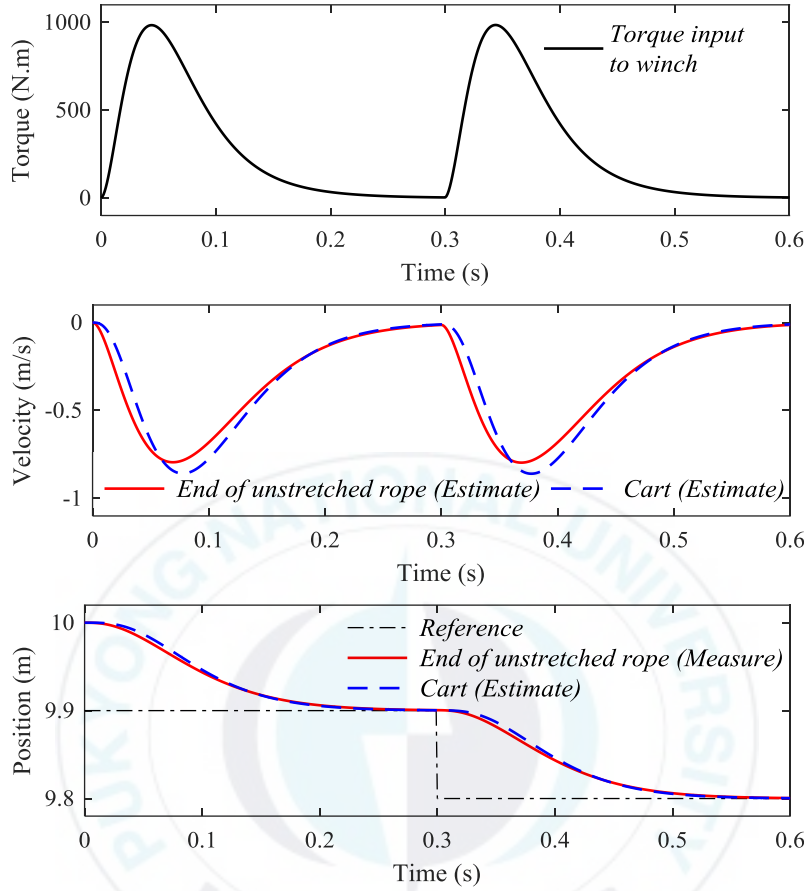
, and these values give the observer gain vector of Eq. (2.23).

$$\mathbf{K} = [-5040 \quad -319 \quad 12841]^T \quad (2.23)$$

Simulations with spring and damping parameters for various lengths of rope are performed to evaluate the proposed controller. Fig 2.8 shows simulation results of proposed reduced-order observer servomechanism control. All cases show desirable position tracking performance.



(a) Rope length 20m



(b) Rope length of 10m

Fig. 2.8 Simulation results of proposed reduced-order observer servomechanism control

From top to bottom: input torque to winch; velocity of unstretched rope (\dot{x}_r) and cart (\dot{x}_c); position of unstretched rope (x_r) and cart (x_c)

Another simulation is carried out to check the efficiency of the controller. Here, the responses of the controlled and uncontrolled cases are compared. As demonstrated in Fig. 2.9, in controlled case, the velocity of cart changes smoothly, and the cart can track the reference position. In the uncontrolled case, velocity of cart alters quickly, an abrupt change appears at 0.08 seconds,

and the cart cannot follow the reference input. These results show the desirable performance of the proposed controller.

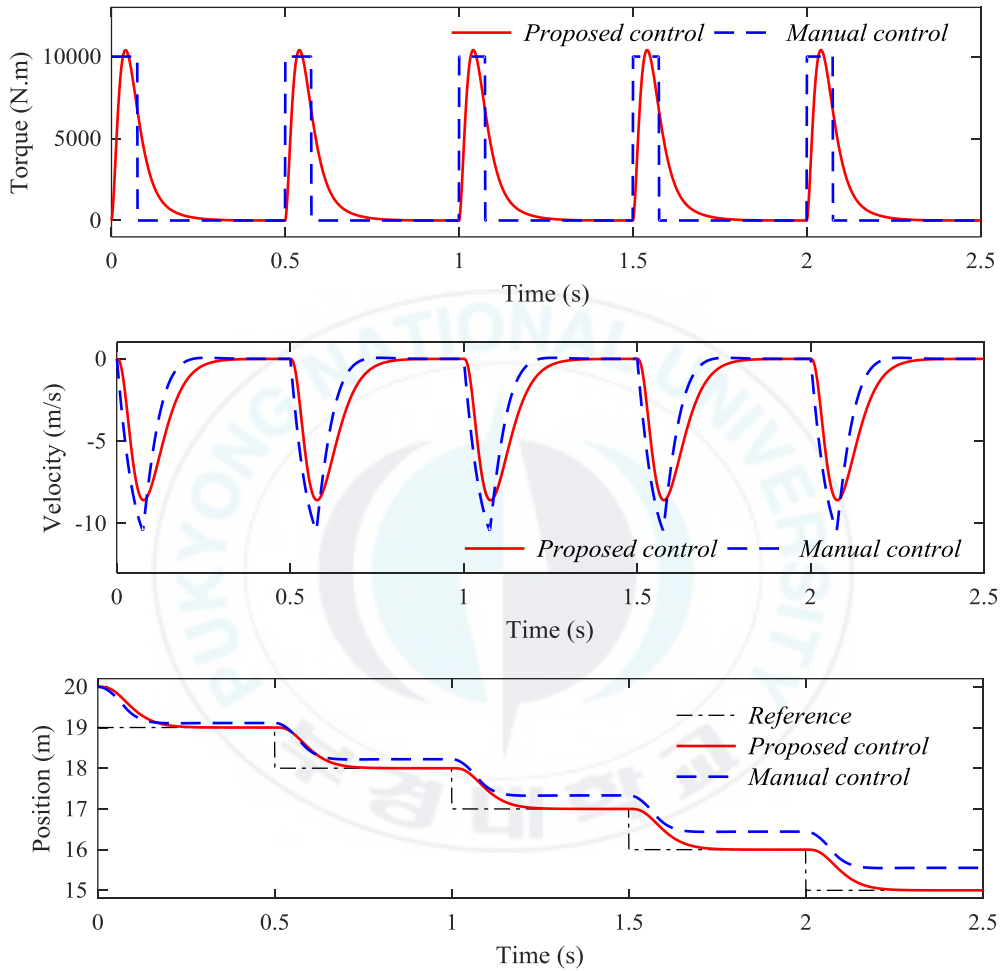


Fig. 2.9 Comparison plots of controlled (proposed control method) and uncontrolled cases

2.4 Summary

This chapter has examined a control-oriented dynamic model of a towing rope system with various lengths. By looking upon varying spring and

damping constants of rope, the changing length of the rope was more accurately modeled. The reduced-order observer-based servomechanism controller was designed using pole placement technique to track the desired motion. It was verified through simulations that the proposed model is effective.



Chapter 3. System Identification and Control Design of Towing Rope System

3.1 Introduction

The first step in control system design is to establish an appropriate mathematical model of the system. In Chapter 2, the state-space representation of the dynamic towing rope system has been well developed. The system model is constructed with rope parameters, i.e. the spring constant k_r and damping constant b_r that depend on changing in length of rope. However, the problem is that these physical parameters are difficult to determine by direct measurements.

In order to overcome the drawback noted above, a family of low-order linear models are estimated from input-output measurements of the towing rope system plant. Then, a 2DOF robust controller is designed and implemented based on the identified model. The workflow consists of steps such as collecting data, estimating linear plant models, designing and simulating 2DOF μ -controller, and implementing the controller on the towing rope system for validating rope tension control strategy.

3.2 Identification of Towing Rope System

3.2.1 System Configuration

The structure of the towing rope system is schematically demonstrated in Fig. 3.1.

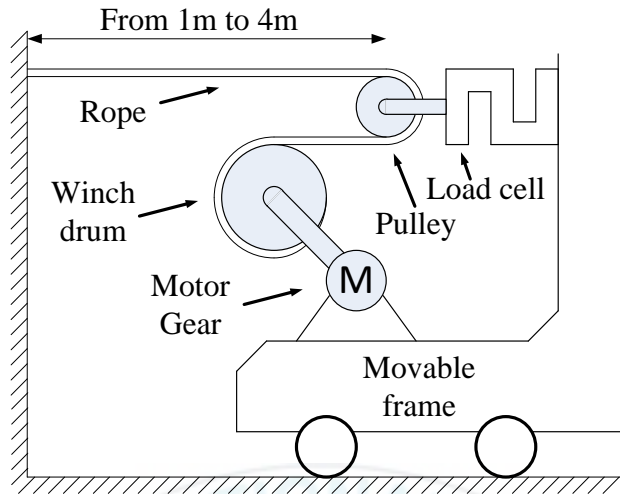


Fig. 3.1 Schematic diagram of towing rope system

The winch system is mounted on the movable frame of the crane system as illustrated in Fig. 3.2.

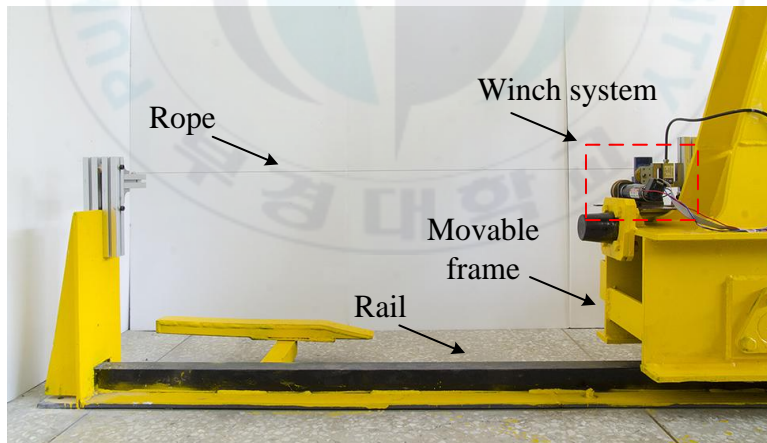
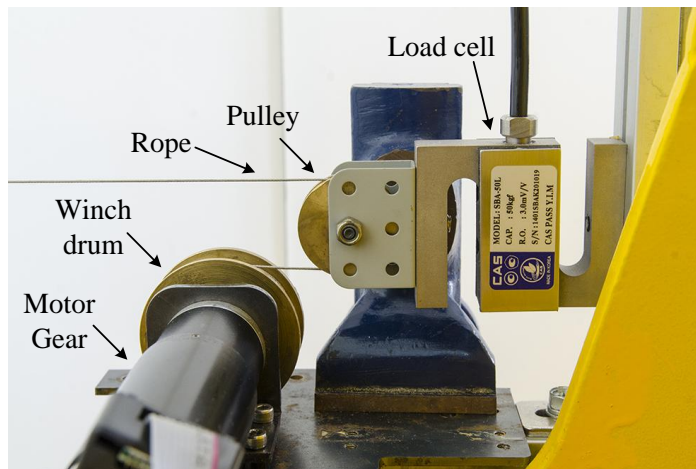


Fig. 3.2 Photo of towing rope system

The winch system illustrated in Fig. 3.3 consists of DC motor, driver, gear, pulley, winch drum, load cell and amplifier.



(a) The winch system



(b) Maxon DC motor
(RE 30 Ø30 mm)



(c) Maxon gearhead
(GP 32 A Ø32 mm)



(d) Maxon motor driver
(ESCON 36/2 DC)



(e) Load cell
(CASKOREA CSBA-100LS)



(f) Amplifier
(CASKOREA LCT-II)

Fig. 3.3 Photos of experimental apparatus

In this experimental setup, a computer installed with NI LabVIEW software and an NI USB-6229 data acquisition device are used to communication and control the DC motor driver as well as load cell amplifier. Fig. 3.4 shows the data acquisition device USB NI-6229.



Fig. 3.4 Photo of data acquisition device USB NI-6229

3.2.2 Data Acquisition

In this step, the sweep sinusoidal chirp signal with variable frequency from 1 Hz to 20 Hz in a sweep time of around 10 seconds was sent to the actuator such that the rope tension was increased and decreased. Control voltage and tension force measured by load cell were logged. Rope length was changed from 1m to 4m, and the corresponding data were collected. Fig. 3.5 shows a sample of experimental data for chirp signal responses of towing rope system.

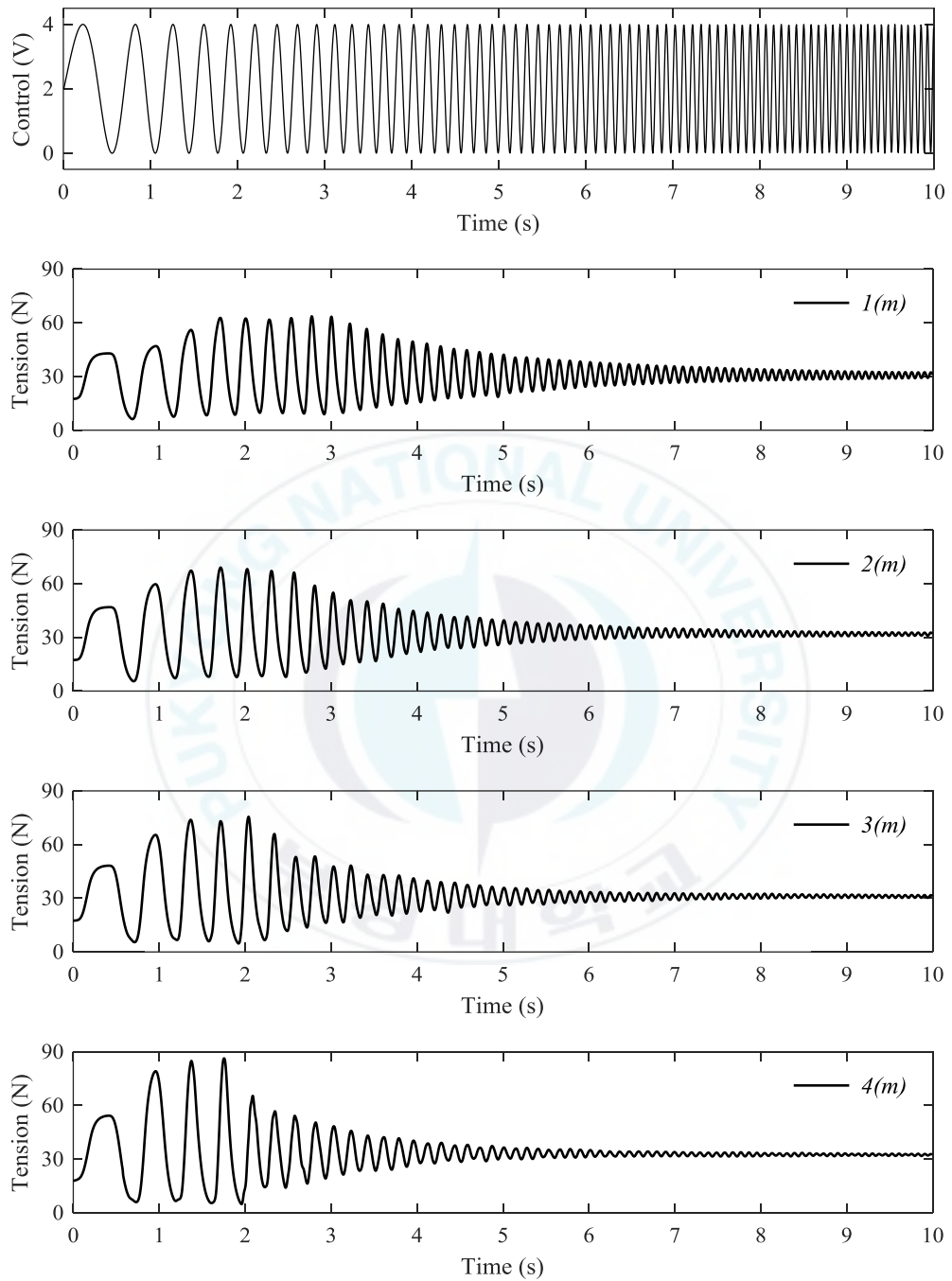


Fig. 3.5 Chirp signal responses of towing rope system

3.2.3 Developed Plant Model

Let's define a basic model of towing rope system as Eq. (3.1).

$$G(s) = \frac{b_0 s^2 + b_1 s + b_2}{s^3 + a_1 s^2 + a_2 s^1 + a_3} \quad (3.1)$$

The linear dynamic models of towing rope system were estimated by using the motor control voltage as an input signal and tension of rope measured by load cell as an output signal. The parameters in Eq. (3.1) were estimated by using MATLAB Identification Toolbox, and summarized in Table 3.1. It is clear that the parameter values strongly depend on rope length variation. Then, we took a nominal model using the nominal values represented in Table 3.1. Based on the nominal values, parameter variations were considered as uncertainties used in designing robust control system.

Table 3.1 Estimated parameter values of towing rope model given in Eq. (3.1)

Length (m)	b_0	b_1	b_2	a_1	a_2	a_3
1	-135.3	2470	50730	20.74	785.2	3240
2	-111.7	1908	39800	18.46	552.1	2430
3	-90.76	1619	28780	14.98	424.3	1816
4	-85.37	1520	19820	12.87	304.2	1180
Minimum	-135.3	1520	19820	12.87	304.2	1180
Maximum	-85.37	2470	50730	20.74	785.2	3240
Nominal	-110.3	1995	35275	16.8	544.7	2210
Variation [%]	23	24	44	23	44	47

3.2.4 Uncertainty Analysis

From the above results, the nominal transfer function of the towing rope system was taken as third-order model of Eq. (3.2).

$$\bar{G}(s) = \frac{\bar{b}_0 s^2 + \bar{b}_1 s + \bar{b}_2}{s^3 + \bar{a}_1 s^2 + \bar{a}_2 s + \bar{a}_3} \quad (3.2)$$

where parameters are given in Table 3.2.

Table 3.2 Nominal parameter of towing rope transfer function

\bar{b}_0	\bar{b}_1	\bar{b}_2	\bar{a}_1	\bar{a}_2	\bar{a}_3
-110.3	1995	35275	16.8	544.7	2210

Notice that a parameter with a bar above denotes its nominal value.

It is found that the actual gain coefficients b_0, b_1, b_2, a_1, a_2 and a_3 are constants with relative errors of 23%, 24%, 44%, 23%, 44% and 47%, respectively. The uncertain frequency responses of the towing system are shown in Fig. 3.6.

In order to account unmodeled dynamics and nonlinear effects, the uncertainty in the towing rope system was approximated by input multiplicative uncertainty that gave rise to the perturbed transfer function [67-68] of Eq. (3.3).

$$G = \bar{G}(1 + W_\Delta \Delta) \quad (3.3)$$

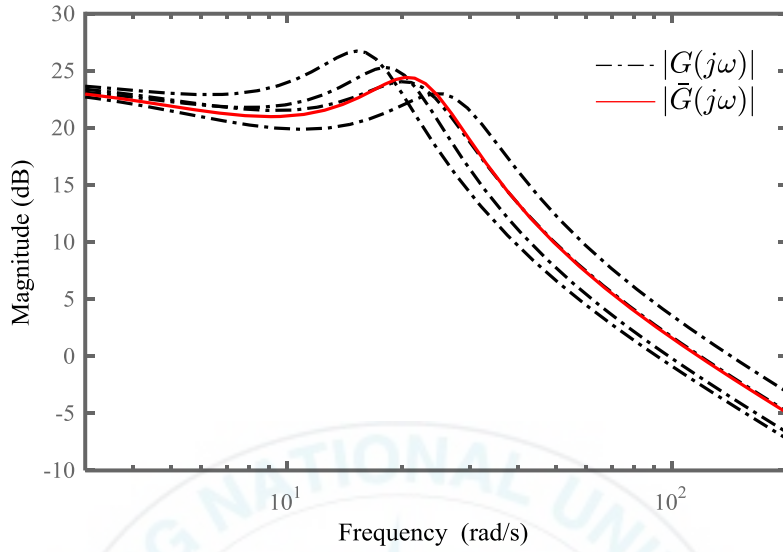


Fig. 3.6 Uncertain frequency responses of the towing rope system

where all uncertainty was concentrated in the unmodeled dynamics Δ , and the gain of Δ was uniformly bounded by 1 at all frequencies with $\Delta \leq 1$. The uncertainty weighting function W_Δ which was used to capture how the relative amount of uncertainty varies with frequency was chosen as Eq. (3.4).

$$\frac{|G(j\omega) - \bar{G}(j\omega)|}{|\bar{G}(j\omega)|} < |W_\Delta(j\omega)| \quad (3.4)$$

The frequency response of W_Δ was graphically found as shown in Fig. 3.7, and then approximated by first-order transfer function. As a result, we obtained Eq. (3.5).

$$W_\Delta = \frac{1.172s + 0.5238}{0.8s + 8.791} \quad (3.5)$$

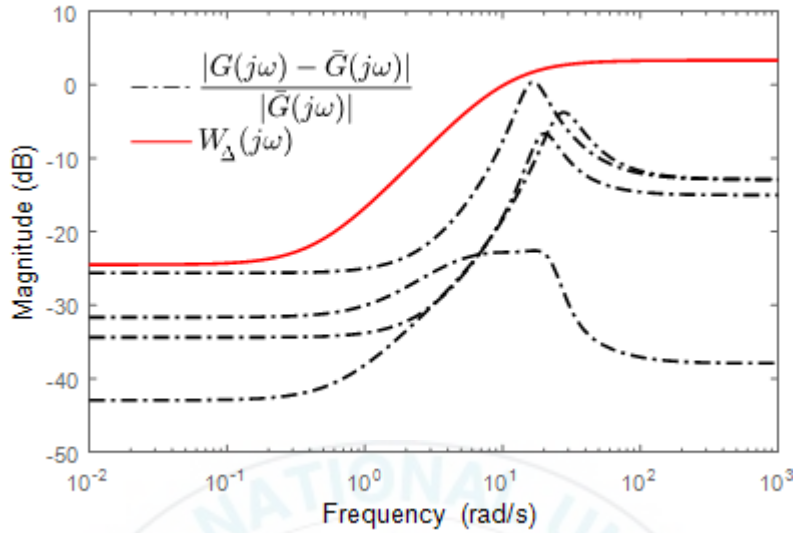


Fig. 3.7 Towing rope system uncertainty approximation

The block diagram of the towing rope system with input multiplicative uncertainty is shown in Fig. 3.8.

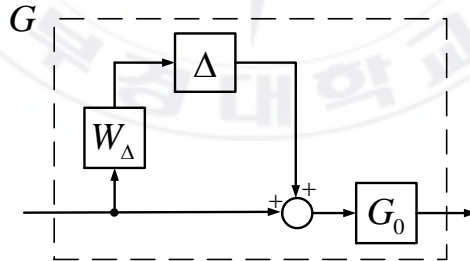


Fig. 3.8 Block diagram of the perturbed towing rope system

3.3 Robust Control Design

3.3.1 Design Specifications

The block diagram of the closed-loop system is depicted in Fig. 3.9. The towing rope system model, the feedback structure and the controller, as well

as the elements reflecting the model uncertainty and the performance objectives are included in this diagram. The plant enclosed by the dashed rectangle contains the nominal towing rope system model \bar{G} with the input multiplicative uncertainty.

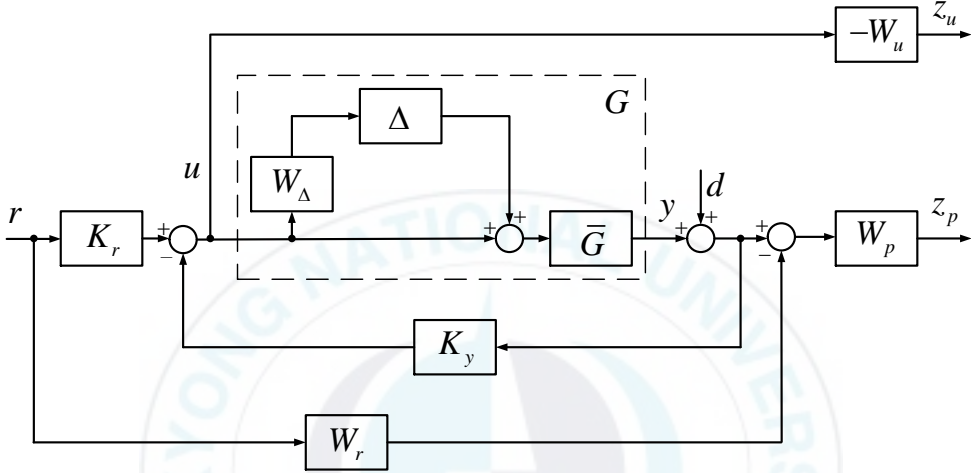


Fig. 3.9 Interconnection structure of the closed-loop system

The system has a reference input r , an input disturbance d , a control signal u and two output costs z_p and z_u . The appropriately chosen weighting functions W_p and W_u are used to reflect the relative significance over different frequency ranges for which the performance is required. The model W_r is an ideal dynamics model to which the designed closed-loop system has to match.

In order to achieve better performance, we present the design of a 2DOF controller that ensures robust stability and robust performance of the closed-loop system. The idea of the 2DOF scheme is to use a feedback controller K_y to achieve the internal robust stability and disturbance rejection, and to

design another controller K_r on the feedforward path to meet the tracking requirement which minimizes the difference between the output of the overall system and that of the reference model. In the given case, the controller K consists of K_y and K_r , and it is represented as $K = [K_r \ -K_y]$. It is easy to show that

$$\begin{bmatrix} z_p \\ z_u \end{bmatrix} = \begin{bmatrix} W_p(-W_r + SGK_r) & W_p(I + T) \\ -W_u(I + K_y G)^{-1} K_r & -W_u(I + K_y G)^{-1} K_y \end{bmatrix} \begin{bmatrix} r \\ d \end{bmatrix}. \quad (3.6)$$

where $S = (I + GK_y)^{-1}$ is the sensitivity function, and $T = (I + GK_y)^{-1} GK_y$ is the complementary sensitivity function for the towing rope system model. The performance objectives are to satisfy

$$\left\| \begin{bmatrix} W_p(-W_r + SGK_r) & W_p(I + T) \\ -W_u(I + K_y G)^{-1} K_r & -W_u(I + K_y G)^{-1} K_y \end{bmatrix} \right\|_{\infty} < 1 \quad (3.7)$$

for each uncertain G .

The weighting functions W_p and W_u are used to reflect the relative significance of the performance requirement over different frequency ranges. In the given case, the performance weighting function is a scalar function, and it is chosen as Eq. (3.8).

$$W_p = \frac{0.5s + 3}{s + 0.0003} \quad (3.8)$$

The control weighting function W_u is chosen simply as the scalar $W_u = 6$, and ideal system model are chosen as Eq. (3.9).

$$W_r = \frac{1}{0.3s + 1} \quad (3.9)$$

3.3.2 Open-loop and Closed-loop System Interconnections

The internal structure of the four-input, five-output open-loop system is shown in Fig. 3.10.

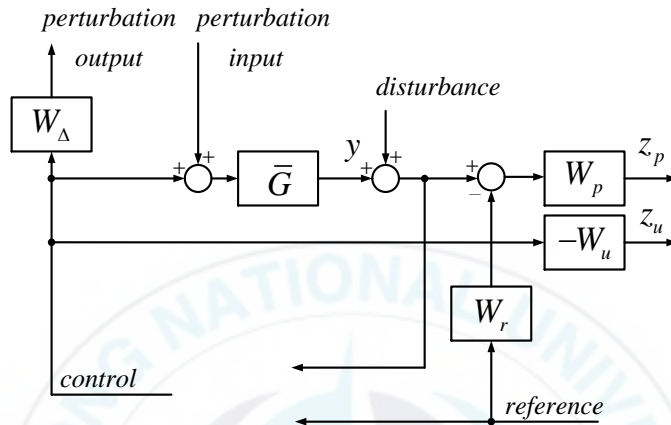


Fig. 3.10 Open-loop interconnection structure of the towing rope system

The block diagram used in the simulation of the closed-loop system is shown in Fig. 3.11.

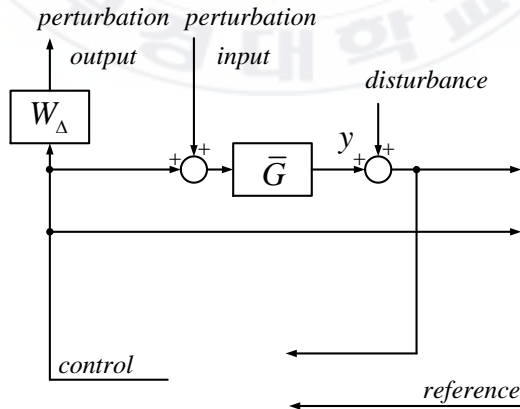


Fig. 3.11 Closed-loop interconnection structure of the towing rope system

3.3.3 μ -Synthesis

The block diagram of the closed-loop system used in the μ -synthesis is shown in Fig. 3.9. Let $P(s)$ denotes the transfer function matrix for the open-loop system with the four inputs and five outputs open-loop system consisting of the towing rope system model with the weighting functions, and let the block structure Δ_P be defined as Eq. (3.10).

$$\Delta_P := \begin{bmatrix} \Delta & 0 \\ 0 & \Delta_F \end{bmatrix} \quad (3.10)$$

The first block of this matrix corresponds to the uncertainty block Δ used in modelling the uncertainty of the towing rope system. The second block Δ_F is a fictitious uncertainty 2×2 block introduced to include the performance objectives in the framework of the μ -approach. To meet the design objectives, a stabilizing controller K is to be found such that at each frequency $\omega \in [0, \infty]$ the structured singular value satisfies the condition of Eq. (3.11).

$$\mu_{\Delta_P}[F_L(P, K)(j\omega)] < 1 \quad (3.11)$$

The fulfillment of this condition guarantees robust performance of the closed-loop system for Eq. (3.12).

$$\left\| \begin{bmatrix} W_p(-W_r + SGK_r) & W_p(I + T) \\ -W_u(I + K_y G)^{-1}K_r & -W_u(I + K_y G)^{-1}K_y \end{bmatrix} \right\|_{\infty} < 1 \quad (3.12)$$

The μ -synthesis is done by using M-file *dkit* from the MATLAB Robust Control Toolbox which automates the procedure by using D-K iterations. The progress of the D-K iteration is shown in Table 3.3.

Table 3.3 Results of the μ -synthesis

Iteration	Controller order	Maximum value of μ
1	7	3.455
2	7	1.239
3	11	0.943

As can be seen from Table 3.3, after the third D-K iteration, an appropriate controller of order 11 is obtained, and the maximum value of μ is equal to 0.943. The controller frequency responses are shown in Fig. 3.12.

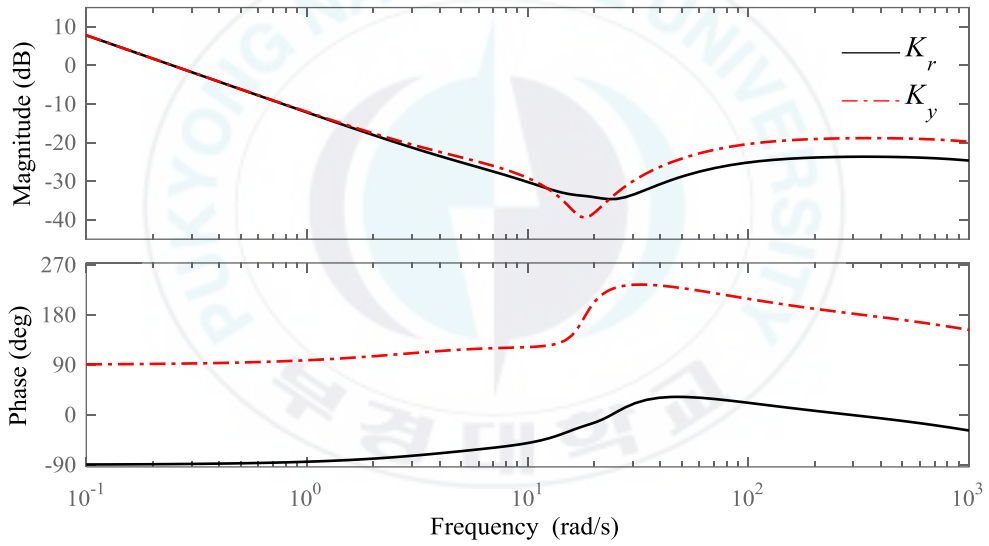


Fig. 3.12 Frequency responses of the controller

3.3.4 Order Reduction of μ -Controller

The order of the μ -controller is 11 which makes it difficult to implement. A reduced-order controller would be usually preferred. In this case study, the Hankel-norm approximation is used and implemented. First, approximations of various orders are generated, and then robust performance margin for each

reduced-order approximation is computed. The robust performance margin measures how much uncertainty can be sustained without degrading performance, and a margin of one or more indicates that we can sustain 100% of the specified uncertainty. Fig. 3.13 shows relation between controller order and robust performance margin.

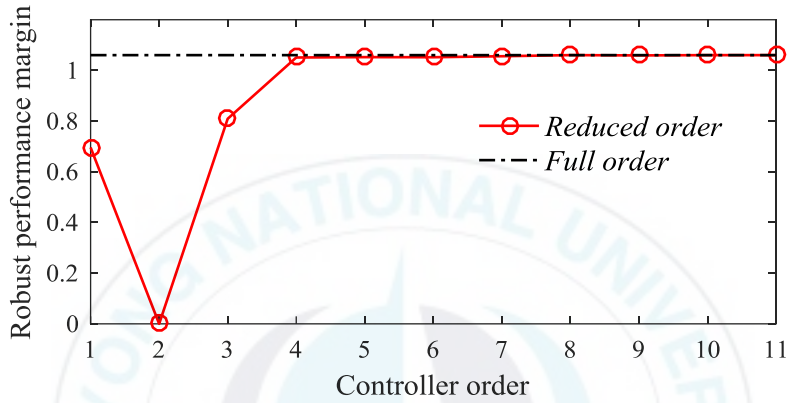


Fig. 3.13 Relation between controller order and robust performance margin

As can be seen from the Fig. 3.13, there is no significant difference in robust performance margin between the 4th and 11th order controllers. Therefore, 4th order approximation is chosen to safely replace synthesized controller using Eq. (3.13).

$$K_r = \frac{99.85s^3 + 2524s^2 + 54880s + 253200}{s^4 + 1537s^3 + 113500s^2 + 1031000s + 309.2} \quad (3.13)$$

$$K_y = \frac{-175.4s^3 - 2071s^2 - 66270ss - 253200}{s^4 + 1537s^3 + 113500s^2 + 1031000s + 309.2}$$

This simplified controller provides robust control with a balance between passenger comfort and handling. In Fig. 3.14 we compare the Bode plots of

the full order with reduced-order controllers. The corresponding plots practically coincide with each other which implies similar performance of the closed-loop systems.

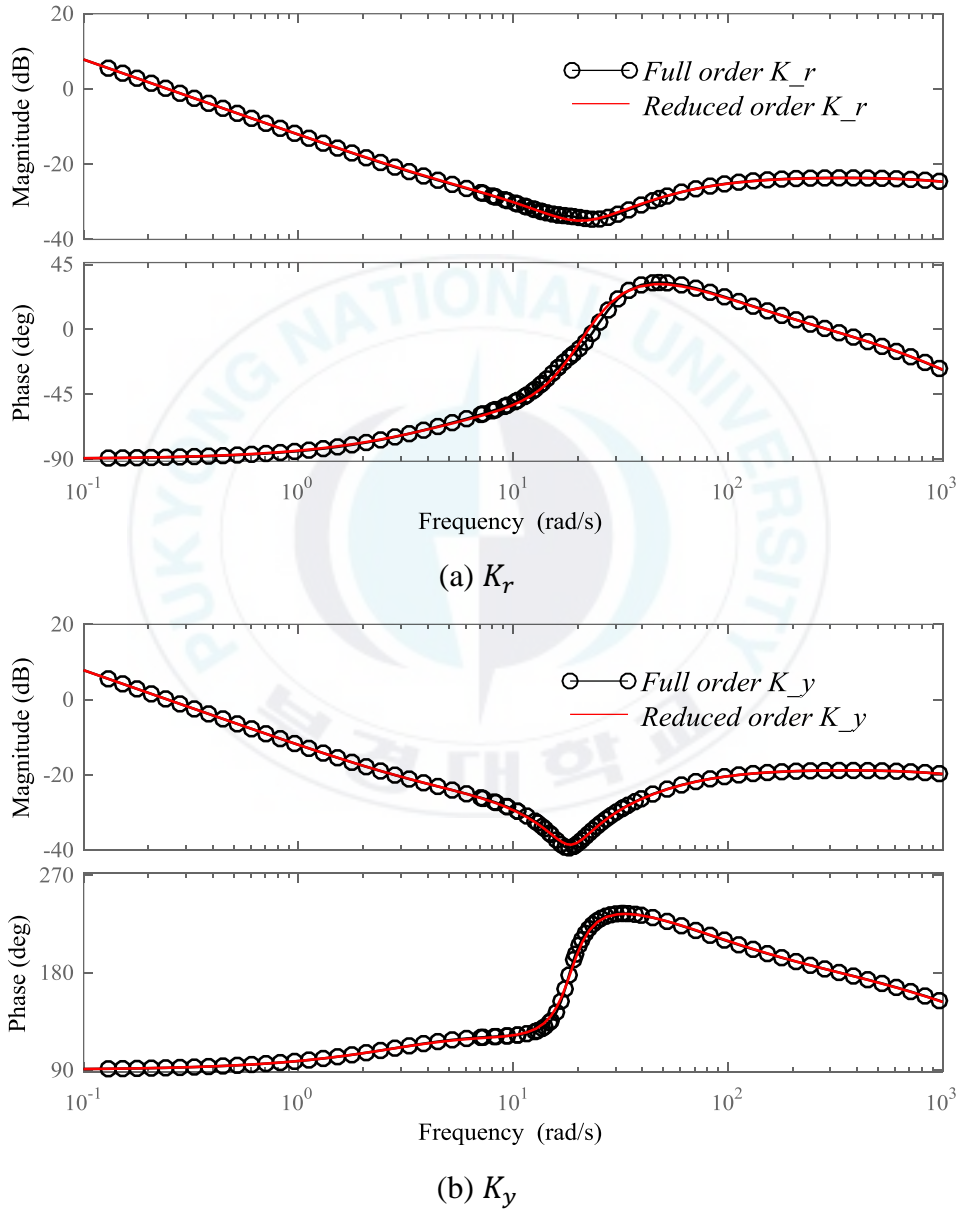


Fig. 3.14 Bode plots of full and reduced-order controllers

3.3.5 Analysis of Closed-loop System

The upper and lower bounds of the structured singular value μ in the case of robust stability analysis are shown in Fig. 3.15.

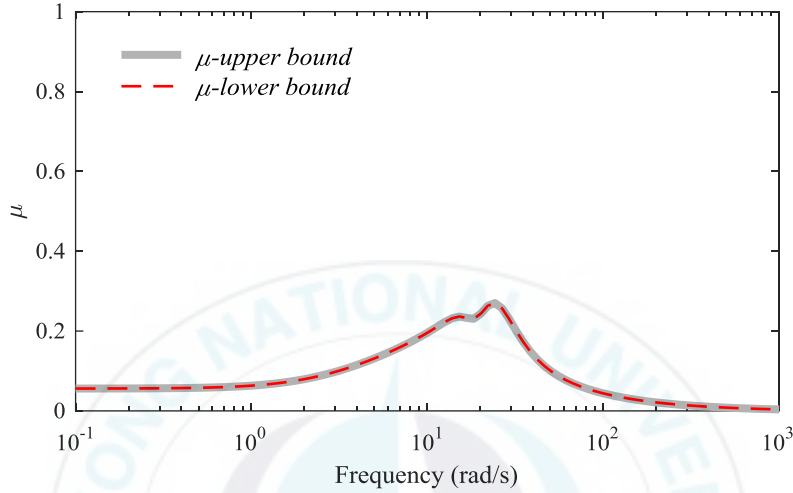


Fig. 3.15 Robust stability for 2DOF controller

The maximum value of μ is 0.27, which means that the stability of the system is preserved under perturbations that satisfies Eq. (3.14).

$$\|\Delta\|_{\infty} < \frac{1}{0.27} \quad (3.14)$$

The frequency response of μ for the case of robust performance analysis is shown in Fig. 3.16. The closed-loop system achieves robust performance, and the maximum value of μ is equal to 0.951 [67].

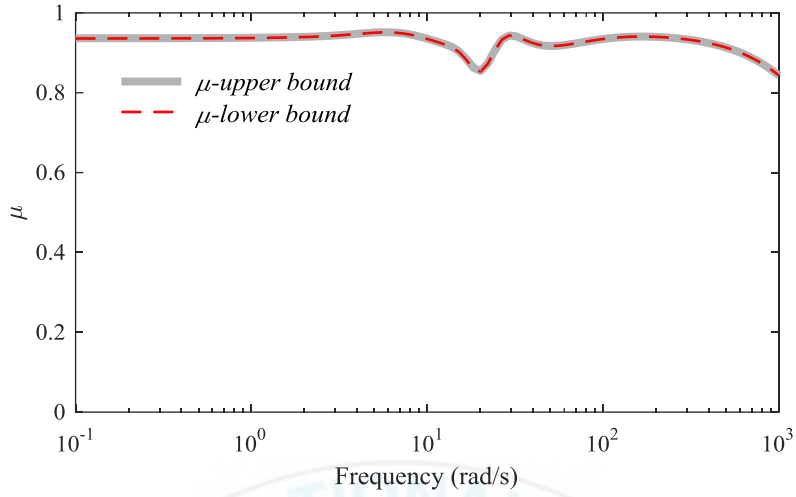


Fig. 3.16 Robust performance for 2DOF controller

3.4 Experimental Results

In this study, two control methods (PID and robust control) were applied to evaluate the proposed control strategy and its performance. In PID control scheme, the following PID controller was introduced into Eq. (3.15).

$$K_{PID} = K_P + K_I \frac{1}{s} + K_D \frac{K_N}{1 + K_N \frac{1}{s}} \quad (3.15)$$

with

$$K_P = 0.0148,$$

$$K_I = 0.1626,$$

$$K_D = -0.003,$$

$$K_N = 3.0391$$

The robust controller was calculated in Eq. (3.13). The simulation results of transient responses with respect to the step reference input and to the step disturbance input of the controllers are shown in Fig. 3.17.

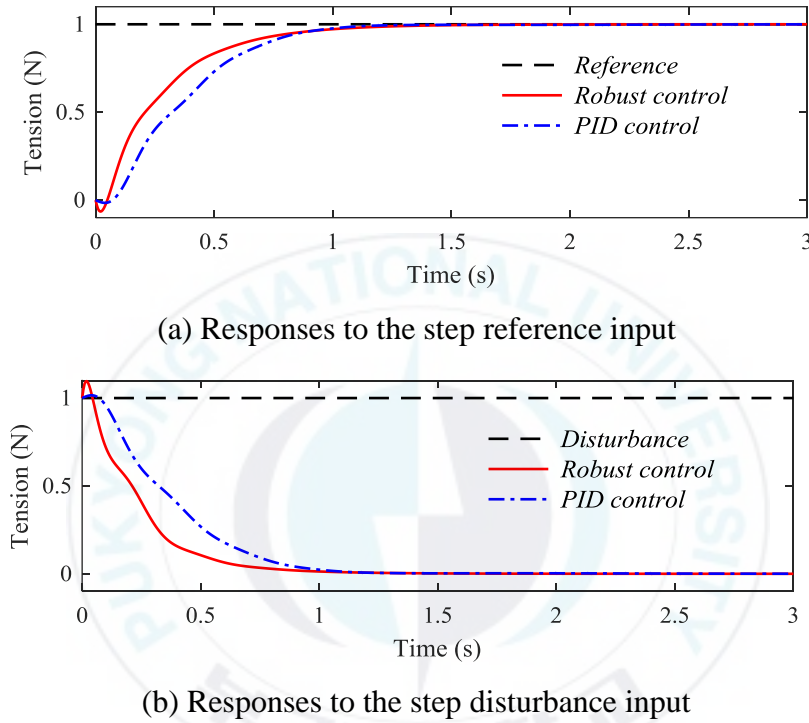


Fig. 3.17 Transient responses of the robust and PID controller

Based on the above results, we evaluated the proposed method. It is obvious that both control methods can track the target route and thus to prove the effectiveness of the proposed identification and control design. However, we can find out that the control performance of robust control strategy is better than that of PID control. The root-mean-square error (RMSE) values were calculated and shown in Table 3.4. From the results we can note that the robust control system gives smaller error and better control performance

than PID control's. Fig. 3.18 shows the control performances of two control methods at the rope length of 3m.

Table 3.4 Root-mean-square error [N]

Rope length \	1 m	2 m	3 m	4 m
Robust control	1.6708	1.8311	2.1523	2.2270
PID control	2.2469	2.7372	2.6811	3.1458

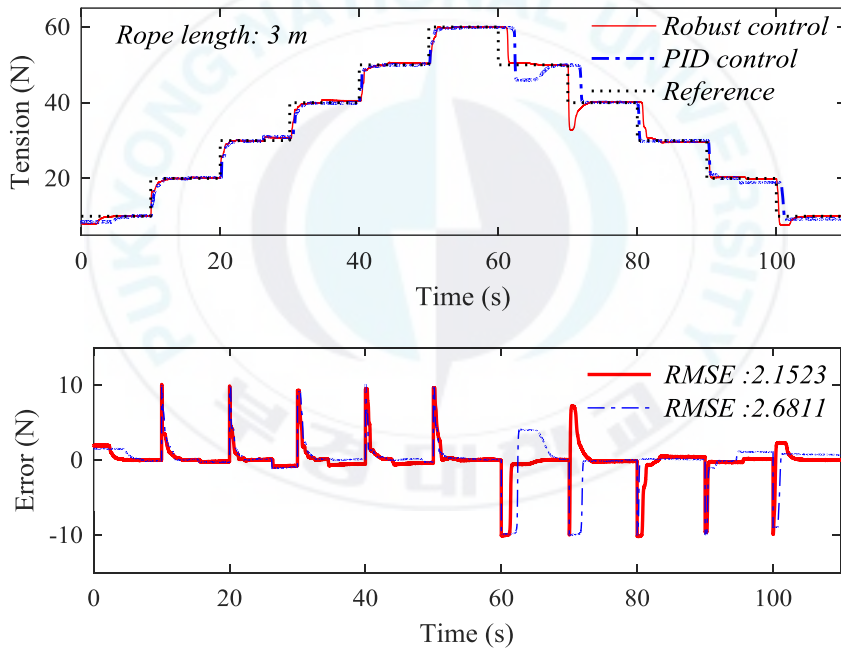


Fig. 3.18 Reference tracking and error for rope length of 3m

3.5 Summary

In this chapter, a 2DOF μ -synthesis robust controller for towing rope system was developed to ensure the robustness of closed-loop system under

the influence of uncertainty, such as the rope length variation and the unmodeled dynamics of rope model. The simulated and experimental results showed that the proposed control system is able to control tension of towing rope system. In addition, as compared to the traditional PID controller, the proposed controller had better performances.



Chapter 4. Vessel Motion Control using Rope Tension Control Strategy

4.1 Introduction

A rope tension control strategy for controlling vessel motion is presented in this chapter. Assuming that none of the vessel's actuators is used, and the vessel is recognized as being an unactuated system. Four mooring systems are employed to control the movement of the vessel. The mathematical model of the system consisting of the vessel and four mooring systems is proposed. Since system parameters of the vessel model are difficult to measure, many experiments and simulations are carried out to estimate vessel's inertia and damping matrices. Then, a PI controller is designed to keep or maneuver the vessel to desired position. The effectiveness of the proposed controller is evaluated through experimental results.

4.2 Mathematical Modelling

4.2.1 Control Strategy

The previous researches have tended to focus on DP and PM systems assisted by activating propulsion systems. This is due to the fact that the main winch is large size, long and slow operating response, etc. Therefore, the main winch and the mooring ropes are only used for keeping station control without motion control.

In order to solve this problem, it is necessary to apply another control strategy. In this chapter, a new positioning keeping approach is presented. Fig. 4.1 demonstrates the main idea.

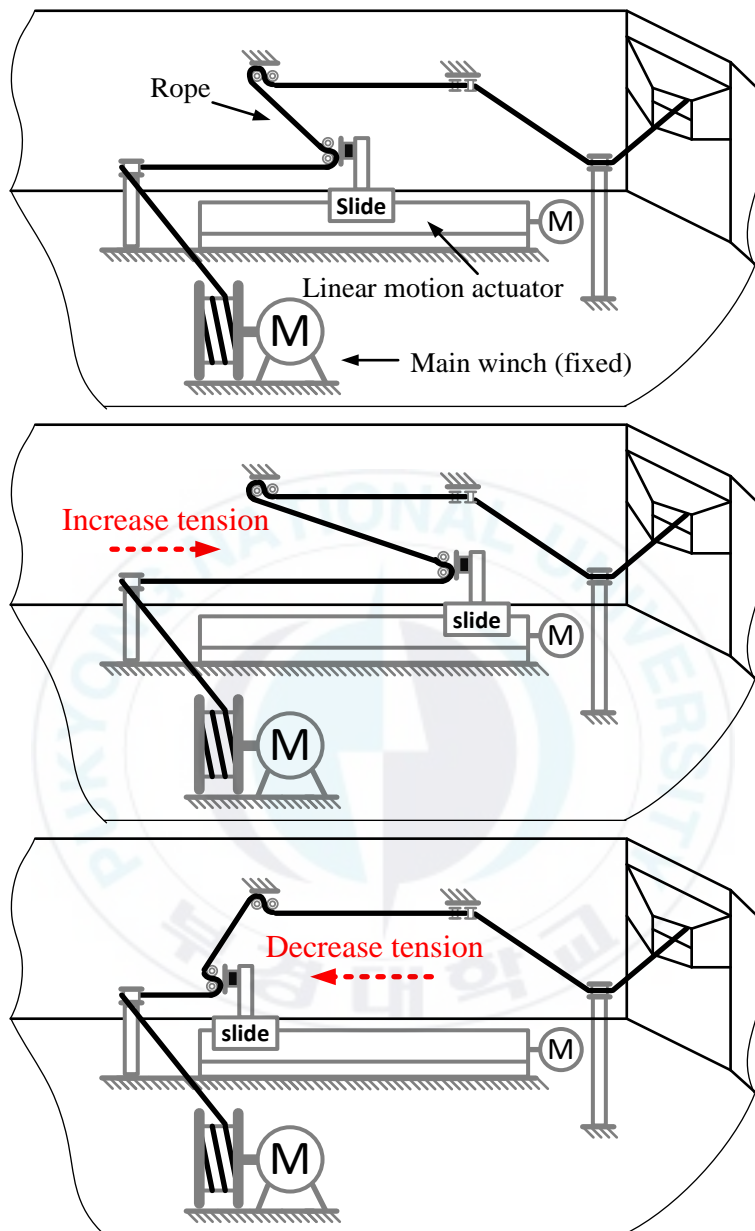


Fig. 4.1 A vessel motion control strategy by using rope tension control

Considering the restraint that the main winch is not employed for the control system, an actuator system is presented, and it can be placed between

the main winch and the rope guide roller. The proposed actuator is actually smaller and faster than the main winch system to achieve good control performance. The rope tension is handled by pulling and releasing the rope without manipulating the main winch in the specified range. The system configuration for this research will be introduced more accurately in the Section 4.4.

4.2.2 Vessel Motion

The floating vessel is usually described by low frequency (LF) and wave frequency (WF) model. The WF model accounts for the motions due to the first-order wave disturbance, whereas the LF model primarily considers the effect of second-order mean and slow varying wave, current, and wind load. However, for anchored vessels, it is assumed that the effect of WF motion is small and can be ignored [69].

The equations of motion in surge, the sway and yaw for the nonlinear LF of the floating vessel are generally given by Eq. (4.1).

$$\begin{aligned}\dot{\boldsymbol{\eta}} &= \mathbf{R}(\psi)\mathbf{v} \\ \mathbf{M}\dot{\mathbf{v}} + \mathbf{C}_{RB}(\mathbf{v})\mathbf{v} + \mathbf{C}_A(\mathbf{v}_r)\mathbf{v}_r + \mathbf{D}(\mathbf{v}_r)\mathbf{v}_r + \mathbf{G}(\boldsymbol{\eta}) \\ &= \boldsymbol{\tau}_{wave2} + \boldsymbol{\tau}_{wind} + \boldsymbol{\tau}_{moor} + \boldsymbol{\tau}_{thr}\end{aligned}\tag{4.1}$$

where $\boldsymbol{\eta} = [x, y, \psi]^T \in R^3$ represents inertial position (x, y) and heading angle ψ in the earth-fixed coordinate frame, and $\mathbf{v} = [u, v, r]^T \in R^3$ describes the surge, sway and yaw rate of ship motion in the body-fixed coordinate frame. The rotation matrix in heading direction $\mathbf{R}(\psi)$ describes the kinematic of motion by Eq. (4.2).

$$\mathbf{R}(\psi) = \begin{bmatrix} \cos \psi & -\sin \psi & 0 \\ \sin \psi & \cos \psi & 0 \\ 0 & 0 & 1 \end{bmatrix} \quad (4.2)$$

The relative velocity vector considering the effect of current is defined as Eq. (4.3).

$$\mathbf{v}_r = [u - u_c, v - v_c, r]^T \quad (4.3)$$

and the current components are calculated by Eq. (4.4).

$$u_c = V_c \cos(\beta_c - \psi), v_c = V_c \sin(\beta_c - \psi) \quad (4.4)$$

where V_c and β_c are the velocity and direction angle of the surface current, respectively. $\mathbf{M} \in R^{3 \times 3}$ is inertia matrix of the LF system including the added mass as described as Eq. (4.5).

$$\mathbf{M} = \begin{bmatrix} m - X_{\dot{u}} & 0 & 0 \\ 0 & m - Y_{\dot{v}} & -Y_{\dot{r}} \\ 0 & -N_{\dot{v}} & I_z - N_{\dot{r}} \end{bmatrix} \quad (4.5)$$

where m is the vessel mass, and I_z is the inertia moment for the vessel in fixed z-axis. For control application, the vessel motion is restricted to low frequency. The wave frequency is assumed to be independent of added inertia which implies $\dot{\mathbf{M}} = 0$.

$\mathbf{C}_{RB}(\mathbf{v}) \in R^{3 \times 3}$ and $\mathbf{C}_A(\mathbf{v}_r) \in R^{3 \times 3}$ are the skew-symmetric Coriolis, and centripetal matrices of the rigid body and the added mass. $\mathbf{D}(\mathbf{v}_r) \in R^{3 \times 3}$ is the damping matrix, and it is a function of the relative velocity \mathbf{v}_r between the vessel and the current defined as Eq. (4.6).

$$\mathbf{D}(\mathbf{v}_r) = \begin{bmatrix} -X_{\tilde{u}} & 0 & 0 \\ 0 & -Y_{\tilde{v}} & -Y_r \\ 0 & -N_{\tilde{v}} & -N_r \end{bmatrix} \quad (4.6)$$

where $\tilde{u} = u - u_c$ and $\tilde{v} = v - v_c$.

The generalized restoring vector $\mathbf{G}(\boldsymbol{\eta}) \in R^3$ caused by the buoyancy and gravitation just affected by heave, roll, and pitch motion is neglected in horizontal motion.

In station keeping application, where the velocity of ship is assumed to be small, and then $\mathbf{C}_{RB}(\mathbf{v})\mathbf{v} + \mathbf{C}_A(\mathbf{v}_r)\mathbf{v}_r$ can be ignored, and $\mathbf{D}(\mathbf{v}_r)$ is assumed to be constant [32], [55] and rewritten as Eq. (4.7).

$$\mathbf{D} = \begin{bmatrix} -X_u & 0 & 0 \\ 0 & -Y_v & -Y_r \\ 0 & -N_v & -N_r \end{bmatrix} \quad (4.7)$$

$\boldsymbol{\tau}_{wave2}$, $\boldsymbol{\tau}_{wind}$, $\boldsymbol{\tau}_{moor}$ and $\boldsymbol{\tau}_{thr}$ are second-order wave disturbance, wind, mooring, and thruster vectors, respectively.

4.2.3 Multi-rope Mooring System Dynamics

The mooring system includes a number of mooring ropes, each rope is attached at one end to the vessel via a winch system, and the other end is fixed to the sea floor by anchor. Normally, the mooring rope is subjected to three types of excitation such as large amplitude LF motion, medium amplitude WF motion and small amplitude with very high-frequency vortex-induced vibration [70]. In the PM system design, it is simplified by considering the influence due to the LF motion on the mooring ropes and ignoring the effect caused by high-frequency vortex-induced vibration. Thus,

the horizontal model for the generalized mooring force is expressed in Eq. (4.8).

$$\boldsymbol{\tau}_{moor} = -\mathbf{R}^T(\psi)\mathbf{g}_{moor}(\boldsymbol{\eta}) - \mathbf{d}_{moor}(\mathbf{v}) \quad (4.8)$$

where $\mathbf{d}_{moor} \in R^3$ is the additional damping, and $\mathbf{g}_{moor} \in R^3$ is the earth-fixed restoring force due to the mooring system. The earth-fixed restoring force is a combination of tensions produced from the mooring ropes given by Eq. (4.9).

$$\mathbf{g}_{moor} = \mathbf{T}(\boldsymbol{\alpha})\mathbf{F} \quad (4.9)$$

where $\mathbf{T}(\boldsymbol{\alpha}) \in R^{3 \times N}$ is the mooring rope configuration matrix, and $\mathbf{F} \in R^N$ is the resultant horizontal force from N mooring ropes. Then, this matrix can be defined as Eq. (4.10).

$$\mathbf{T}(\boldsymbol{\alpha}) = \begin{bmatrix} \cos \alpha_1 & \dots & \cos \alpha_N \\ \sin \alpha_1 & \dots & \sin \alpha_N \\ x_1 \sin \alpha_1 - y_1 \cos \alpha_1 & \dots & x_N \sin \alpha_N - y_N \cos \alpha_N \end{bmatrix} \quad (4.10)$$

where x_i, y_i and α_i are moment arms and angle between mooring line and x -axis of vessel as shown in Fig. 4.2.

The force produced at each mooring rope is the function of the horizontal distance between the attached point and the anchor point of the rope and the rope length. Using the elastic catenary equations [70] or some marine software packages, the horizontal rope tension component at end upper end can be calculated.

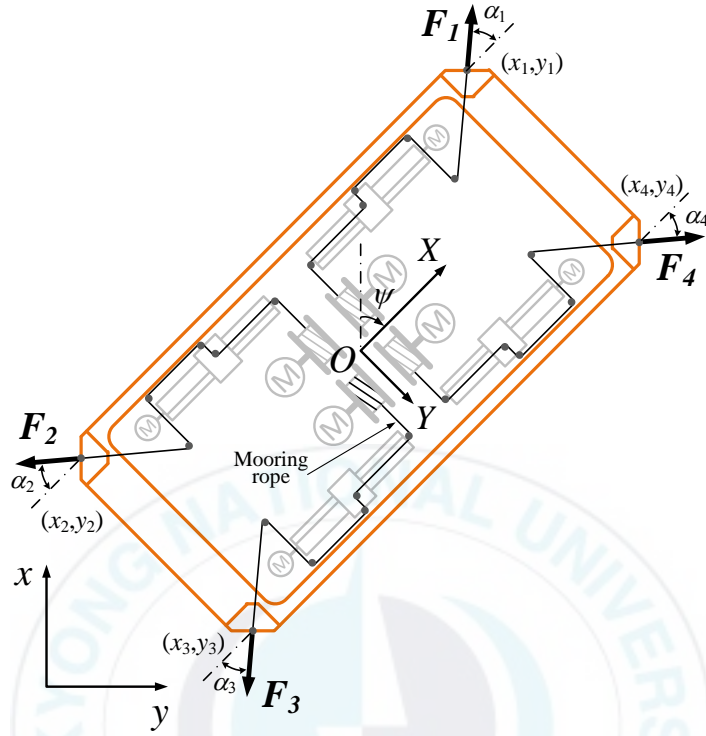


Fig. 4.2 Mooring rope configuration in vessel motion control

4.3 Controller Design

The main object of most mooring systems is to control the slowly varying LF motions of the vessel encounter with wind, wave and current. In this research, the mooring system produces a reactive force to compensate for the mean drift loads of the environment due to environment disturbances, and to keep the vessel in station. The vessel position is controlled by changing the rope tension. This is done by winches equipped on the vessel to pull in or let out the ropes.

To do this, a high-level plant controller which calculates the command surge, sway forces and yaw moment is needed. In this study, a PI controller

is introduced to solve this problem. The integral component eliminates the steady state error between the desired position and current position of the vessel. The equation of the controller can be described as Eq. (4.11) [69].

$$\boldsymbol{\tau}_c = \mathbf{R}^T(\psi) \left(\mathbf{K}_P(\boldsymbol{\eta}_d - \boldsymbol{\eta}) + \mathbf{K}_I \int_0^t (\boldsymbol{\eta}_d - \boldsymbol{\eta}) d\tau \right) \quad (4.11)$$

where $(\boldsymbol{\eta}_d - \boldsymbol{\eta}) \in R^3$ is the position error, $\boldsymbol{\eta}_d \in R^3$ is the desired position, $\boldsymbol{\eta} \in R^3$ is the current position of the vessel, and $\mathbf{K}_P, \mathbf{K}_I \in R^{3 \times 3}$ is the proportional and integral gain matrices, respectively. The control strategy is illustrated in Fig. 4.3.

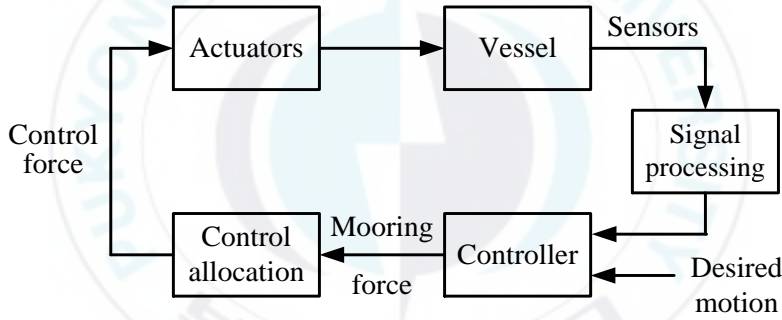


Fig. 4.3 Block diagram of control strategy

In the next step, the generalized control forces $\boldsymbol{\tau}_c \in R^3$ in surge, sway and yaw are distributed to the mooring system. This is the mooring rope allocation problem. The relationship between the generalized control force vector and the resultant horizontal forces from N mooring ropes \mathbf{F} is given by Eq. (4.12).

$$\boldsymbol{\tau}_c = \mathbf{T}(\alpha)\mathbf{F} \quad (4.12)$$

Normally, the mooring system of a vessel includes from 4 to 16 mooring ropes. Thus, the mooring rope configuration matrix $\mathbf{T}(\boldsymbol{\alpha}) \in R^{3 \times N}$ may not be a square matrix, and computation of \mathbf{F} from $\boldsymbol{\tau}_c$ is a model-based optimization problem. In this study, the command control action provided by the mooring ropes is calculated by using an explicit method. The solution of this method to the Least Square Optimization problem using Lagrange Multipliers is introduced by Fossen [69]. Therefore, the solution horizontal force vector of N mooring ropes is obtained as Eq. (4.13).

$$\mathbf{F} = \mathbf{T}^+(\boldsymbol{\alpha})\boldsymbol{\tau}_c \quad (4.13)$$

where $\mathbf{T}^+(\boldsymbol{\alpha}) \in R^{N \times 3}$ is the pseudo inverse of the mooring rope configuration matrix.

4.4 Experiment

The experiments were carried out in the Marine Cybernetics Laboratory located at the Department of Control and Mechanical System Engineering, Pukyong National University using the model vessel. The vessel has a mass of 215 kg, length of 2 m and breath of 1 m, and it uses is a 1:50 scaled model of the barge type vessel.

4.4.1 System Identification

By running the experiments without currents or exogenous disturbances and assuming that the vessel has homogeneous mass distribution, xz and yz plane symmetry as well as center of gravity coincides with center of geometry, and the vessel model is described as Eq. (4.14).

$$\mathbf{M}\dot{\mathbf{v}} + \mathbf{D}\mathbf{v} = \boldsymbol{\tau}$$

$$\mathbf{M} = \begin{bmatrix} m - X_{\ddot{u}} & 0 & 0 \\ 0 & m - Y_{\ddot{v}} & 0 \\ 0 & 0 & I_z - N_{\ddot{r}} \end{bmatrix}$$

$$\mathbf{D} = \begin{bmatrix} -X_u & 0 & 0 \\ 0 & -Y_v & 0 \\ 0 & 0 & -N_r \end{bmatrix}$$
(4.14)

where the parameters in the system inertia matrix \mathbf{M} and the damping matrix \mathbf{D} must be identified, and $\boldsymbol{\tau} = [\tau_x, \tau_y, \tau_\psi]$ is the input vector of forces in surge, and sway and moment in yaw direction. The mathematical equations for system identification process are described as Eq. (4.15).

$$\begin{cases} (m - X_{\ddot{u}})\ddot{u} + (-X_u)u = \tau_x \\ (m - Y_{\ddot{v}})\ddot{v} + (-Y_v)v = \tau_y \\ (I_z - N_{\ddot{r}})\ddot{r} + (-N_r)r = \tau_\psi \end{cases}$$
(4.15)

The vessel was pulled in surge, sway and yaw direction at different pulling forces, and for each run the force τ_x, τ_y and moment τ_ψ , and the position x, y, ψ were measured and recorded. In order to measure the pulling forces, the load cells were installed on the vessel as shown in Fig. 4.4. One sample data for pulling the vessel in surge direction is presented in Fig 4.5.

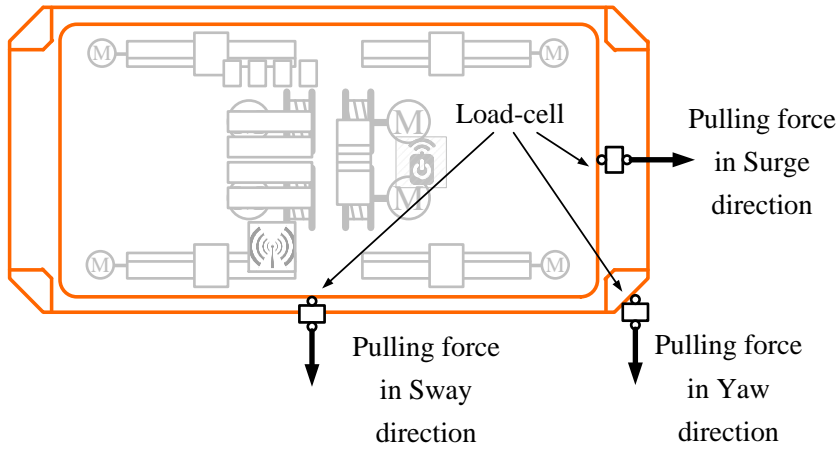


Fig. 4.4 Pulling vessel and measurement set-up for applied forces with load cells

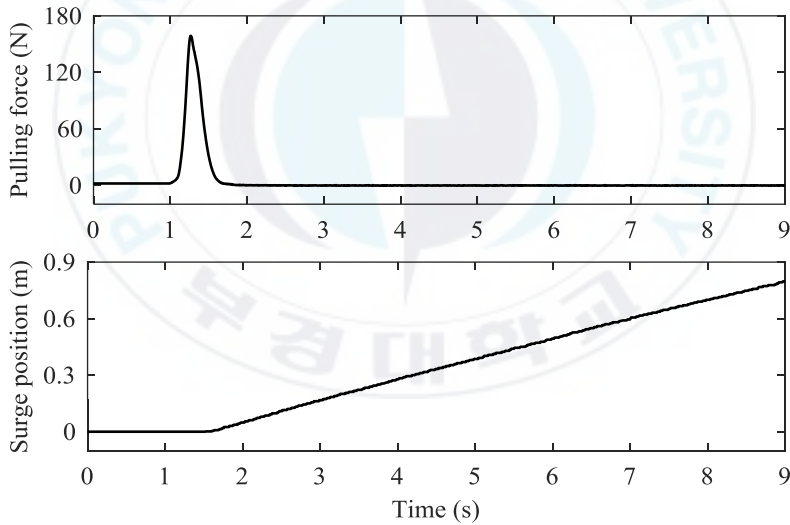


Fig. 4.5 Obtained pulling force and vessel position

In surge direction, simulation model was built based on the pure surge motion equation of $(m - X_{\ddot{u}})\dot{u} + (-X_u)u = \tau_x$. After that, unknown parameters $\{(m - X_{\ddot{u}}), (-X_u)\}$ were estimated by using least square fitting technique. Fig. 4.6 shows the experiment and simulation data for applying a

pulling force of 160 (N) in surge direction. The same process was implemented to estimate unknown parameters in sway and yaw direction of $\{(m - Y_{\dot{v}}), (-Y_v)\}$ and $\{(I_z - N_{\dot{r}}), (-N_r)\}$.

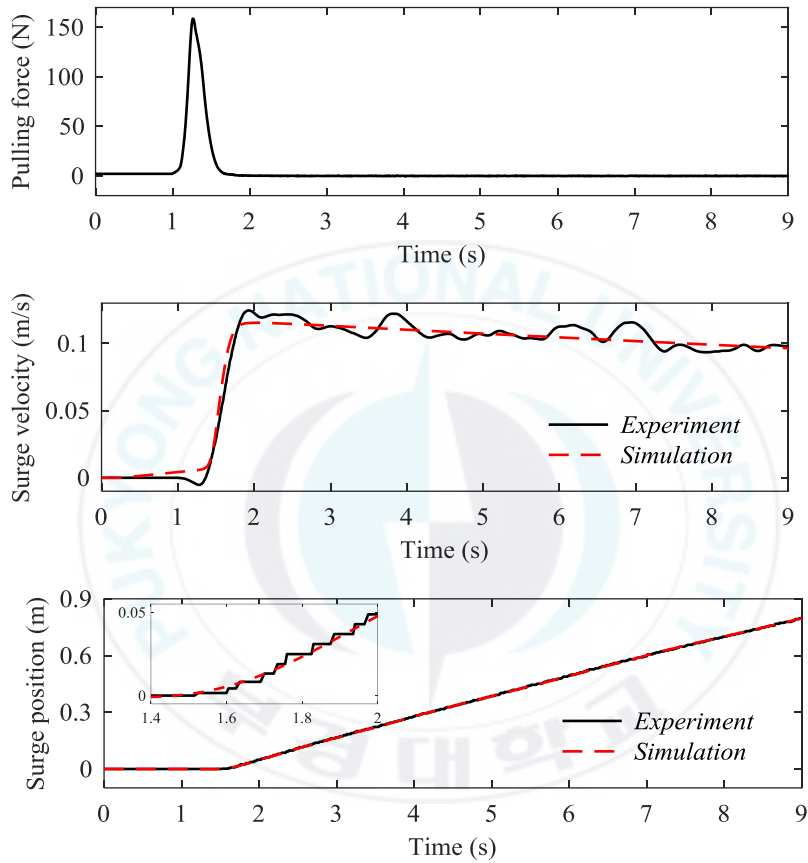


Fig. 4.6 Position and velocity data fitting results

To obtain reliable and accurate data, experiments of more than 10 times were performed. The numerical values with a specific range are summarized in Table 4.1.

Table 4.1 Obtained data from experiments and simulations

x-direction (surge)	$348.5 < m - X_{\dot{u}} < 356$ $8 < -X_u < 14.4$
y-direction (sway)	$294 < m - Y_{\dot{v}} < 372$ $10.27 < -Y_v < 15.07$
z-axis (yaw)	$106.5 < I_z - N_{\dot{r}} < 121.5$ $4.62 < -N_r < 12.6$

As a result, the system inertia matrix \mathbf{M} and damping matrix \mathbf{D} were obtained as shown in Eq. (4.16).

$$\mathbf{M} = \begin{bmatrix} 351.2 & 0 & 0 \\ 0 & 332.4 & 0 \\ 0 & 0 & 113.2 \end{bmatrix} \quad (4.16)$$

$$\mathbf{D} = \begin{bmatrix} 11.44 & 0 & 0 \\ 0 & 12.17 & 0 \\ 0 & 0 & 7.36 \end{bmatrix}$$

4.4.2 Experimental Results

The experimental set-up including the vessel and mooring ropes is shown in Fig. 4.7.

Four ropes were connected to the vessel at four vessel corners to simulate the effect of the mooring system. Each rope has one end attached to the actuator equipped in the vessel and the other to the wall of the basin.

The linear motion actuators were used to obtain required rope tensions by changing the length of ropes. The information of the linear motion actuator system is shown in Fig. 4.8.

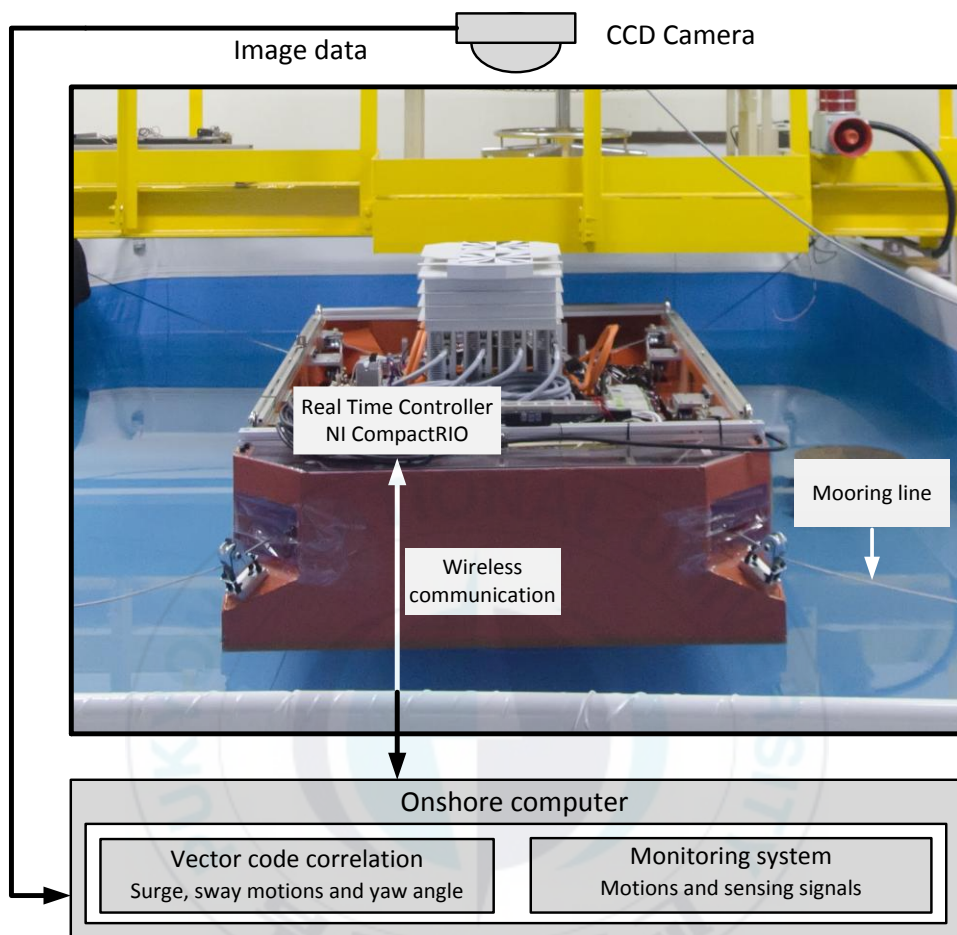


Fig. 4.7 An overview of components for vessel motion control system



(a) Festo spindle axes EGC-80-300-BS-10P-KF-OH-ML-GK



(b) Festo motor
EMME-AS



(c) Festo motor controller
CMMP-AS-C2-3A-M0

Fig. 4.8 Photos of linear motion actuator system

In addition, a mass was suspended between these two ends. The rope tension measurement system consists of a load-cell and an amplifier as shown in Fig 4.9.

The vessel motions were captured by the CCD camera, and it was attached on the ceiling as detailed in Fig. 4.10. The image data obtained by the CCD camera was transferred to the host computer, and the surge, sway positions, and yaw angle were measured by using the vector code correlation

technique in real time [71]. Then the calculated positions and yaw angle were sent to the control system (NI CompactRio) placed on the vessel.



(a) Load cell

(CASKOREA CSBA-100LS)



(b) Amplifier

(CASKOREA LCT-II)

Fig. 4.9 Photos of tension measurement system

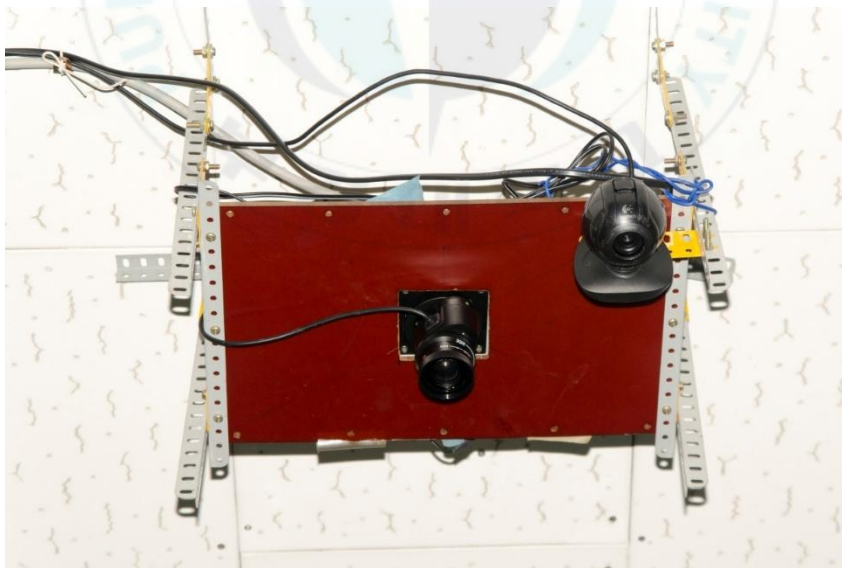


Fig. 4.10 Photo of ceiling CCD camera system

The overview of control system (NI CompactRio) placed on the vessel is shown in Fig. 4.11.



Fig. 4.11 Photo of real-time controller NI cRIO-9024 and modules

Also, all the information including vessel motions and all the sensing signals were transferred to the monitoring system by the wireless network. Fig. 4.12 demonstrates the process and technique for experiment.

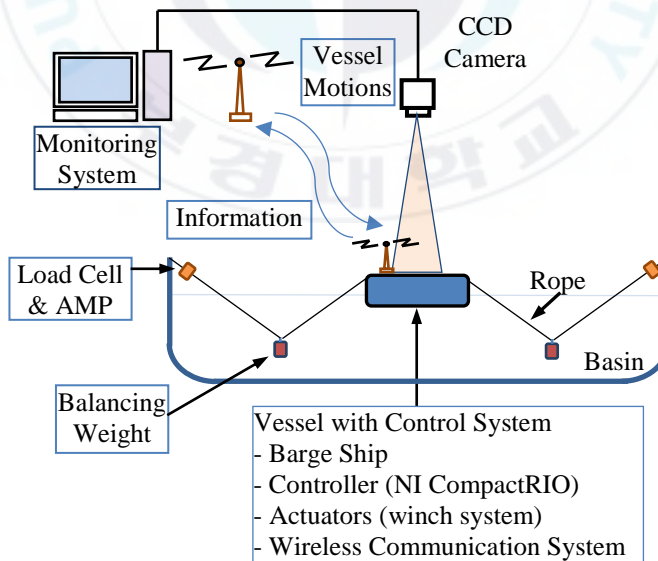


Fig. 4.12 Schematic diagram of experimental set-up

To demonstrate the effectiveness of the controller, first the model was tested without rope tension control. Fig. 4.13 shows the vessel motions in surge, sway and yaw angle. Even though the vessel was slightly restricted by the ropes, it is apparent from this figure that the influence of the wave attack remains for long time.

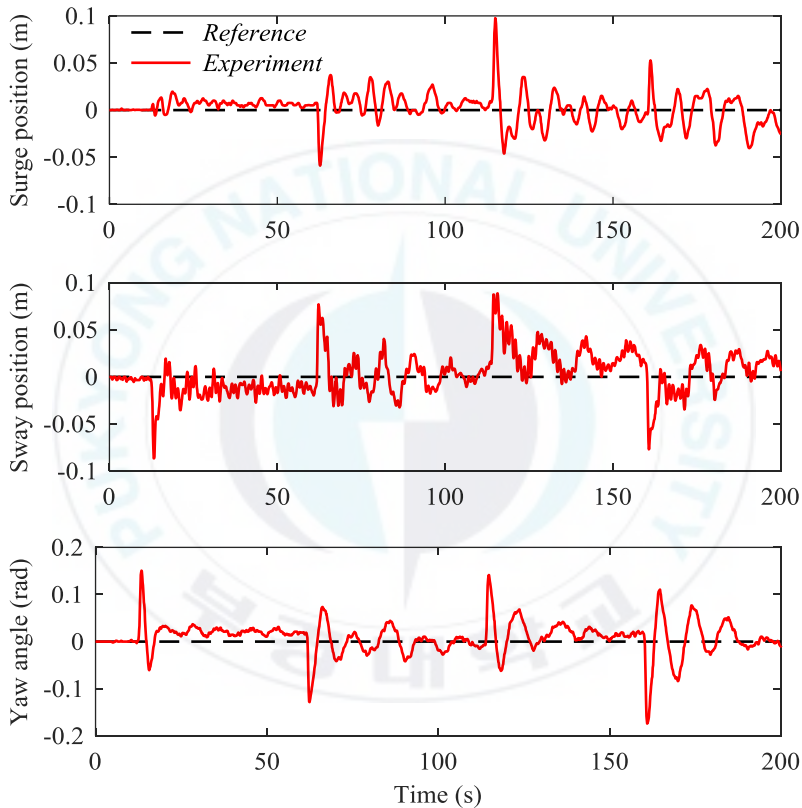


Fig. 4.13 Vessel motions in wave disturbance without control

After that, the rope tension control strategy was applied. The gain matrix K_P and K_I of the PI controller were chosen as Eqs. (4.17) and (4.18).

$$\mathbf{K}_P = \begin{bmatrix} 41.515 & 0 & 0 \\ 0 & 38.755 & 0 \\ 0 & 0 & 13.225 \end{bmatrix} \quad (4.17)$$

$$\mathbf{K}_I = \begin{bmatrix} 0.166 & 0 & 0 \\ 0 & 0.155 & 0 \\ 0 & 0 & 0.053 \end{bmatrix} \quad (4.18)$$

From the Fig. 4.14 we can see that the surge, sway positions and yaw angle return to the initial state in a short time. The result explains that the proposed vessel motion control strategy with PI controller can cope with disturbance.

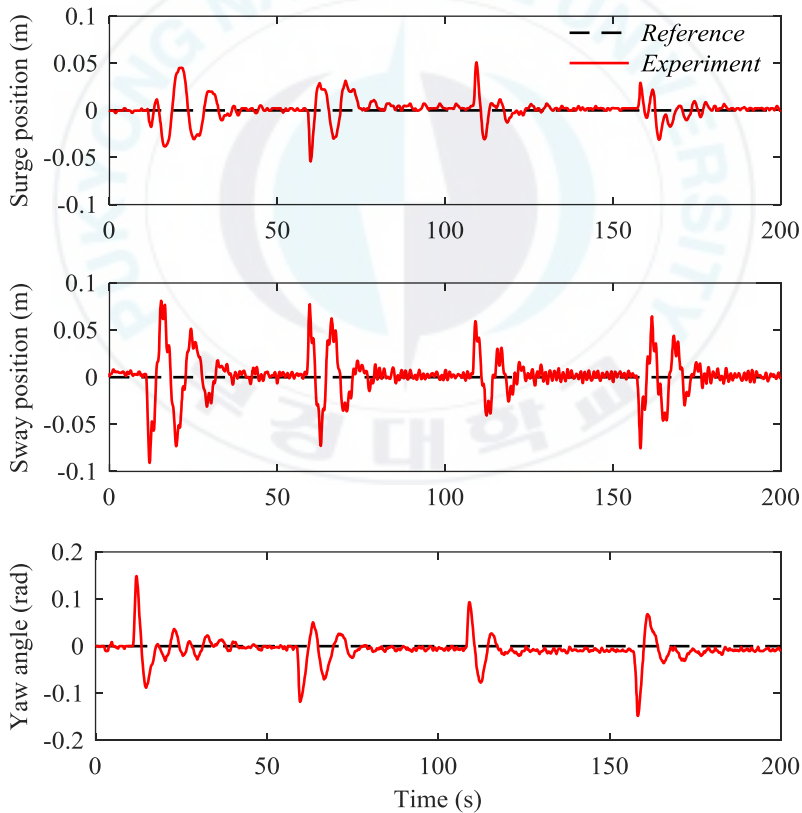


Fig. 4.14 Station keeping experimental results in wave disturbance by using PI control

We also performed other experiments to verify the proposed strategy. For this, position control experiment for two directions was done.

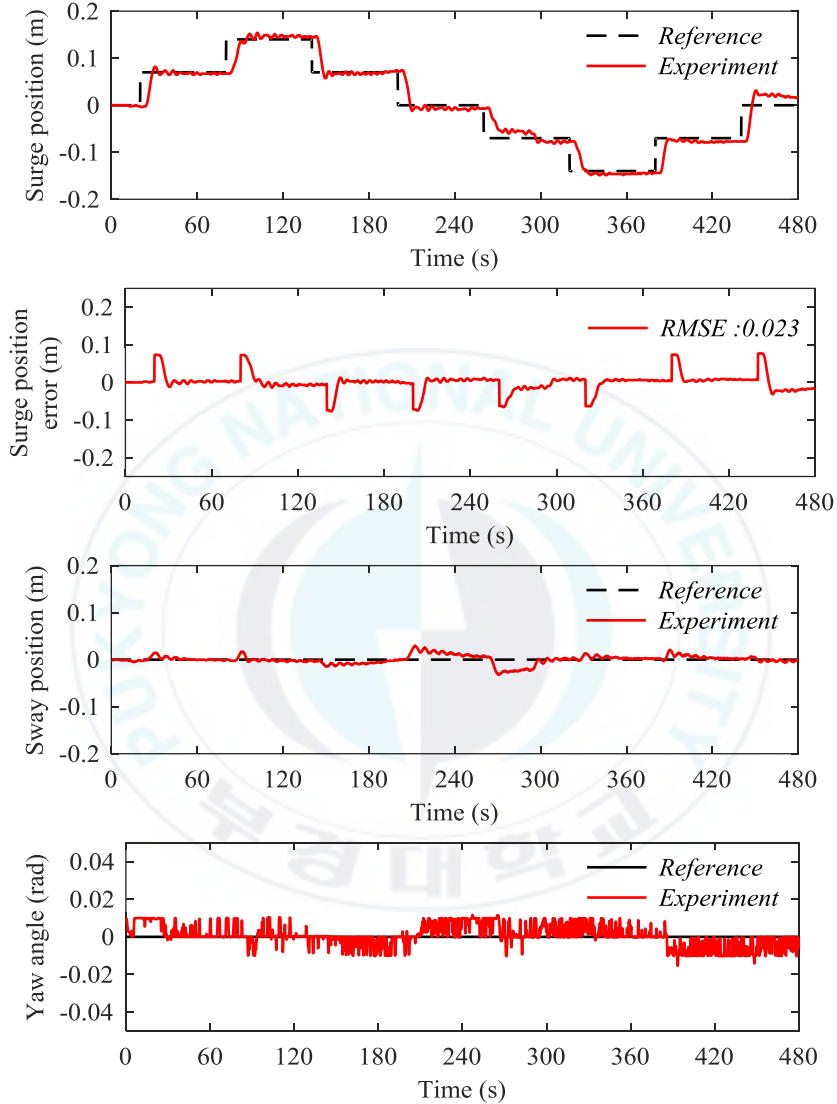


Fig. 4.15 Experimental results for a multi-step reference input in surge direction

In the first case, the vessel has changed location for surge direction in term of every 60s. From the initial position, the vessel moved toward for

positive direction by +7.5cm up to +15cm. Then the vessel returned backward to the initial position by +7.5cm. By changing the moving direction, the same type of position control experiment was operated.

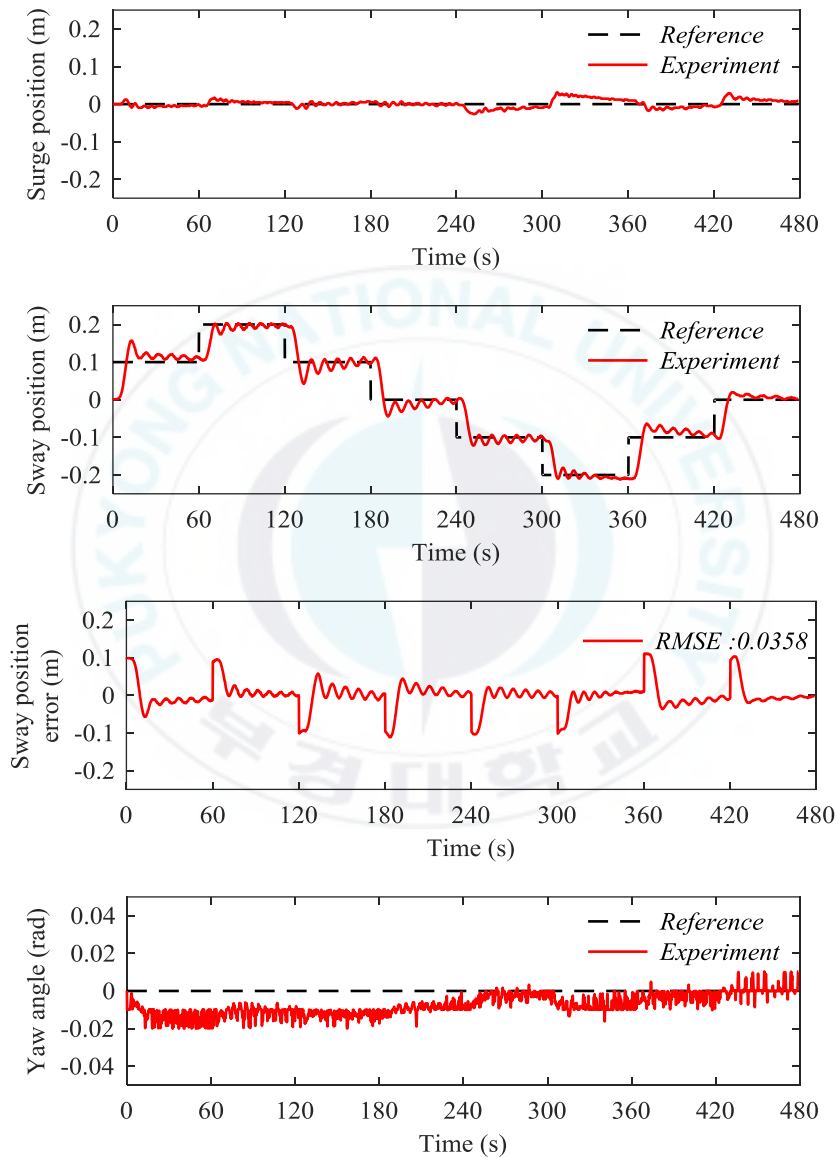


Fig. 4.16 Experimental results for a multi-step reference input in sway direction

The results can be seen in Fig. 4.15-16. It is verified that the vessel moves exactly in the defined position. Finally, it is clear that the proposed control scheme works well and can be used in the real field.

4.5 Summary

This chapter proposed a new strategy for solving the vessel motion control problem. The dynamic motions of the vessel in surge, sway and yaw direction were obtained by regulating the tension of ropes connected to the vessel's linear motion actuators without using any distinct propelling system. In addition, the mathematical model of the barge vessel was identified through the experiment and simulation results.

After that, a PI controller was designed and implemented to control the motion of the vessel. The effectiveness of the proposed controller was evaluated through experimental results. Vessel motions in wave disturbance under active control and uncontrolled operating conditions were considered. The experiments showed that without control, the vessel motions were strongly affected by wave disturbance. However, the surge, sway positions and yaw angle of the vessel with PI controller were maintained at the initial position. Further tests on vessel motion control showed that the designed controller can accurately maneuver the vessel to the desired position. Overall, the implementation of rope tension control strategy on vessel motion control was obtained.

Chapter 5 Conclusion and Future Study

5.1 Conclusion

As stated in the Introduction, the main purpose of this dissertation was to conduct a new strategy for vessel motion control by controlling rope tension. The conclusion of this study was summarized as follows:

In chapter 2, the system modeling of a cart driven by a towing rope system was introduced. Rope characteristics such as spring and damping constant which depend on changing in rope length were considered. As it is well known, the rope motion is hard to measure, and so a reduced-order observer was designed to estimate the motion states of the towing rope system. A 2DOF controller was also derived to make the system track of the desired motion. The proposed controller was evaluated through simulation and comprehensive results.

In chapter 3, the structure of the towing rope system consisting of towing rope and winch system which was mounted on a movable frame was set up. Due to the model-based design method, it strictly requires a system with all known parameters. Unfortunately, it is difficult to determine spring constant and damping constant of towing rope. The system identification technique was applied to overcome this disadvantage. Low-order linear models of the towing rope system were estimated from input-output measurement data. In order to account for unmodeled dynamics and nonlinear effects existed in the towing rope system, the uncertainty was analyzed and approximated by input multiplicative uncertainty. In this study, design method based on the structured singular value μ was used to achieve robust stability and robust

performance. Moreover, a servomechanism design procedure was presented to obtain good control performance. The proposed control method was compared to a PID controller. Both of controllers were evaluated through simulations and experiments. There were no significant differences between the robust controller and PID controller in simulation. However, RMSE values of the robust controller were smaller than that of the PID controller in experiment. This result suggested that the control performance of proposed control method is better than the PID controller's.

In chapter 4, a rope tension control strategy for controlling vessel motion was presented. In the literature, the main winch was not used in vessel motion control due to its large size and slow operating response. In an effort to control motion of vessel without using active propulsion systems, a new control strategy was applied with a smaller and faster actuator placed between the main winch and the rope guiding roller. Pulling or releasing the rope with the actuator would change rope tension. The proposed method was integrated in four mooring systems equipped on an unactuated vessel model. System parameters of vessel were estimated via experiment data. Based on identified vessel model, a PI controller is designed. The effectiveness of the proposed control strategy was validated through overall experiments. The result on station keeping of the vessel with the proposed controller was compared to that of the uncontrolled case. These tests revealed that the proposed vessel motion control with PI controller can cope with disturbance. Further experiments on vessel motion control were conducted. The vessel was maneuvered with multi-step reference input. It was shown that the vessel exactly moved to the defined position. In general, these results would seem to suggest that the proposed control scheme can be applied in the industry field.

5.2 Future Study

Based on the results summarized above, the following future works are listed as a necessary destination:

- Further experimental investigations are needed to measure rope parameters. Thus the control-oriented model of towing rope system introduced in Chapter 2 can be applied in real world situations.
- The combination between towing rope systems and dampers and towing rope systems and tugboats should be studied to solve the berthing problem of vessel in the harbor as illustrated in Fig. 5.1.

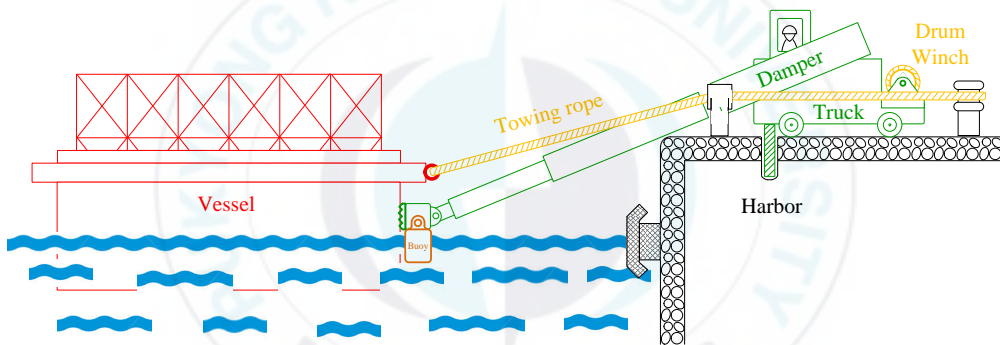


Fig. 5.1 Vessel berthing system assisted by damper and towing rope system

References

- [1] K. Kose, J. Fukudo and K. Sugano, "Study on a Computer Aided Manoeuvring System in Harbors," *Naval Architecture and Ocean Engineering*, vol. 25, pp. 105-113, 1987.
- [2] K. Kose, S. Hirao, K. Yoshikawa and Y. Nakagawa, "Study on Abilities of Harbour Tugboats," *Journal of the Society of Naval of Architects of Japan*, vol. 162, pp. 133-138, 1987.
- [3] K. Ohtsu and T. Takai and H. Yoshihisa "A Fully Automatic Berthing Test Using the Training Ship Shioji Maru," *Journal of Navigation*, vol. 44, no. 2, pp. 213-223, 1991.
- [4] K. Shouji and K. Ohtsu, "A Study on The Optimization of Ship Maneuvering by Optimal Control Theory (1st Report)," *Journal of the Society of Naval of Architects of Japan*, vol. 172, pp. 365-373, 1992.
- [5] K. Shouji and K. Ohtsu, "A Study on The Optimization of Ship Maneuvering by Optimal Control Theory (2nd Report)," *Journal of the Society of Naval of Architects of Japan*, vol. 173, pp. 221-229, 1993a.
- [6] K. Shouji and K. Ohtsu, "A Study on The Optimization of Ship Maneuvering by Optimal Control Theory (3rd Report)," *Journal of the Society of Naval of Architects of Japan*, vol. 174, pp. 339-344, 1993b.
- [7] V.P. Bui, J.S. Jeong, Y.B. Kim and D. Wook, "Optimal Control Design for Automatic Ship Berthing by Using Bow and Stern Thrusters," *Journal of Ocean Engineering and Technology*, vol. 24, no. 2, pp. 10-17, 2010.
- [8] V.P. Bui, H. Kawai, Y.B. Kim, K.S. Lee, "A Ship Berthing System

- Design with Four Tug Boats,” *Journal of Mechanical Science and Technology*, vol. 25, no.5, pp. 1257-1264, 2011.
- [9] T. Takai and H. Yoshihisa, “An Automatic Manoeuvring System in Berthing,” *Proceedings of 8th Ship Control Systems Symposium*, vol. 2, pp. 209-227, 1987.
- [10] Y. A. Kasabeh, M. M. Pourzanjani, M. J. Dove, “Automatic Berthing of Ships,” *Proceeding of the Institute of Marine Engineer 3rd International Conference on Maritime Communications and Control*, pp. 109-116, 1993.
- [11] K. Hasegawa and K. Kitera, “Automatic Berthing Control System using Neural Network and Knowledge-base,” *Journal of Kansai Society of Naval Architects of Japan*, vol. 220, pp.135-143, 1993.
- [12] K. Hasegawa and T. Fukutomi, “On Harbor Maneuvering and Neural Control System for Berthing with Tug Operation,” *Proceeding of 3rd International Conference Manoeuvring and Control of Marine Craft*, pp.197-210, 1994.
- [13] Y. Zhang, G. E. Hearn and P. Sen, “A Multivariable Neural Controller for Automatic Ship Berthing,” *IEEE Journal of Control Systems*, vol. 17, no. 4, pp. 31-45, 1997.
- [14] N. K. Im and K. Hasegawa, “Motion Identification using Neural Networks and Its Application to Automatic Ship Berthing under Wind,” *Journal of Ship and Ocean Technology*, vol. 6, no. 1, pp. 16-26, 2002.
- [15] J. G. Balchen, N. A. Jenssen and S. Saelid, “Dynamic Positioning using Kalman Filtering and Optimal Control Theory,” *IFAC/IFIP Symposium on Automation in Offshore Oil Field Operation*, pp. 183-

186,1976.

- [16] J. G. Balchen, N. A. Jenssen, E. Mathisen and S. Sælid, "A Dynamic Positioning System based on Kalman Filtering and Optimal Control," *Modeling Identification and Control 1*, vol. 3, pp. 135-163, 1980.
- [17] S. Saelid, N. A. Jenssen and J. G. Balchen, "Design and Analysis of a Dynamic Positioning System based on Kalman Filtering and Optimal Control," *IEEE Transactions on Automatic Control*, vol.28, no. 3, pp. 331-339, 1983.
- [18] M. J. Grimbale, R. J. Patton and D. A. Wise, "The Design of Dynamic Ship Positioning Systems Using Extended Kalman Filtering Techniques," *Proceeding of OCEAN'79*, pp. 488-497, 1979.
- [19] M. J. Grimbale, R. J. Patton and D. A. Wise, "The Design of Dynamic Ship Positioning Control Systems Using Stochastic Optimal Control Theory," *Optimal Control Applications and Methods*. vol. 1, no. 2, pp. 167-202, 1980.
- [20] P. T-K. Fung and M. J. Grimbale, "Dynamic Ship Positioning Using Self Tuning Kalman Filter," *IEEE Transaction on Automatic Control*, vol. 28, no. 3, pp. 339-349, 1983.
- [21] Grimbale M. J. and M. A. Jonhson, *Optimal Control and Stochastic Estimation. Theory and Applications*, Wiley, Chichester, USA, 1988.
- [22] T. I. Fossen, *Guidance and Control of Ocean Vehicles*, John Wiley and Sons Ltd, New York, 1994.
- [23] T. I. Fossen and J. P. Strand, "Passive Nonlinear Observer Design for Ships Using Lyapunov Methods: Full-scale experiments with a supply vessel," *Automatica*, vol. 35, no. 1, pp. 3-16, 1999.

- [24] J. P. Strand and T. I. Fossen, "Nonlinear Passive Observer for Ships with Adaptive Wave Filtering," *New Directions in Nonlinear Observer Design* (H. Nijmeijer and Fossen T.I., Eds.), Springer-Verlag, London, Chap. I-7, pp. 113-134, 1999.
- [25] M. R. Katebi, M. J. Grimble and Y. Zhang, " H_∞ Robust Control Design for Dynamic Ship Positioning," *IEE Proceedings – Control Theory and Application*, vol. 144, no.2, pp. 110-120, 1997.
- [26] A. J. Sorensen, S. I. Sagatun and T. I. Fossen, "Design of a Dynamic Positioning System using Model-based Control," *Control Engineering Practice*, vol. 4, no.3, pp. 359-368, 1996.
- [27] E. A. Tannuri, A. C. Agostinho, H. M. Morishita, L. Jr. Moratelli, "Dynamic Positioning Systems: An Experimental Analysis of Sliding Mode Control," *Control Engineering Practice*, vol. 18, no.10, pp. 1121-1132, 2010.
- [28] A. J. Sorensen, S. T. Quek and T. D. Nguyen, "Improved Operability and Safety of DP Vessels using Hybrid Control Concept", *Proceedings of the International Conference on Technology & Operation of Offshore Support Vessels (OSV 2005)*. 20-21 September 2005 - Singapore.
- [29] T. D. Nguyen, A. J. Sorensen and S. T. Quek, "Design of Hybrid Controller for Dynamic Positioning from Calm to Extreme Sea Conditions," *Automatica*, vol. 43, no.5, pp. 768-785, 2007.
- [30] T. D. Nguyen, "Design of Hybrid Marine Control Systems for Dynamic Positioning," Ph. D dissertation, Department of Civil Engineering, National University of Singapore, 2006.
- [31] J. P. Strand, A. J. Sørensen and T. I. Fossen, "Design of Automatic

- Thruster Assisted Position Mooring Systems for Ships,” *Modeling, Identification and Control*, vol. 19, no.2, pp. 61-75, 1998.
- [32] O. M. Aamo and T. I. Fossen, “Controlling Line Tension in Thruster Assisted Mooring Systems,” *Proceeding of the 1999 IEEE International Conference on Control Applications*, Kohala Coast, HI, pp. 1104–1109, 1999.
- [33] P. I. B. Berntsen, B. J. Leira, O. M. Aamo and A. J. Sørensen, “Structural Reliability Criteria for Control of Large-Scale Interconnected Marine Structures,” *In Proceedings of OMAE'04, paper OMAE2004-51350, 23rd International Conference on Offshore Mechanics and Arctic Engineering*, Vancouver, Canada, June 20-25, 2004.
- [34] T. D. Nguyen and A. J. Sorensen, “Setpoint Chasing for Thruster-assisted Position Mooring,” *IEEE Journal of Oceanic Engineering*, vol. 34, no.4, pp. 548- 558, 2009.
- [35] A. Strandhagen, K. Schoenherr, and F. Kobayashi (1950), “The Stability on Course of Towed Ships,” *Transactions of the Society of Naval Architects and Marine Engineers*, vol. 58, pp. 32-46, 1950.
- [36] K. Kijima and K. Varyani, “Wind Effect on Course Stability of Two Towed Vessels,” *Journal of The Society of Naval Architecture of Japan*, vol. 1985, no. 158, pp. 137-148, 1985.
- [37] M. M. Bernitsas and N. S. Kekridis, “Simulation and Stability of Ship Towing,” *International Shipbuilding Progress*, vol. 32, no. 369, pp. 112-123, 1985.
- [38] M. M. Bernitsas and N. S. Kekridis, “Nonlinear Stability Analysis of Ship Towed by Elastic Rope,” *Journal of Ship Research*, vol. 30, no.

2, pp. 136-146, 1986.

- [39] M. L. Lee, "Dynamic Stability of Nonlinear Barge-towing System," *Applied Mathematical Modelling*, vol. 12, no. 12, pp. 693–701, 1989.
- [40] T. Jiang, R. Henn and S. D. Sharma, "Dynamic Behavior of a Tow System under an Autopilot on The Tug," *International Symposium and Workshop on Forces Acting on a Manoeuvring Vessel*, 1998.
- [41] K. Nonaka, T. Haraguchi and T. Nimura, "On the Slewing Motion of a Towed Barge," *4th Pacific Congress on Marine Science and Technology*, vol. 2, pp. 225–230, 1990.
- [42] K. Yukawa, K. Hoshino, S. Hara and K. Yamakawa, "Hydrodynamic Forces Acting on Capsized Vessel with Geometrical Configuration and Its Towing Method," *Journal of The Society of Naval Architecture of Japan*, 191:87–96, 2002. (Japanese)
- [43] A. Fitriadhy and H. Yasukawa, "Course Stability of a Ship Towing System", *Ship Technology Research*, vol. 58, no. 1, pp. 4-23, 2011.
- [44] A. Fitriadhy, H. Yasukawa and K.K. Koh, "Course Stability of a Ship Towing System in Wind," *Ocean Engineering*, vol. 64, pp. 135-145, 2013.
- [45] A. Fitriadhy, H. Yasukawa and A. Maimun, "Theoretical and Experimental Analysis of a Slack Towline Motion on Tug-towed Ship during Turning", *Ocean Engineering*, vol. 99, pp. 95-106, 2015.
- [46] H.K. Yoon, H.S. Lee, J.K. Park and Y.G. Kim, "Dynamic Modeling and Simulation of a Towing Rope using Multiple Finite Element Method", *Journal of Navigation and Port Research*, vol. 36, no. 5, pp.339-347, 2012.

- [47] J. P. Strand, A. J. Sørensen and T. I. Fossen, “Modelling and Control of Thruster Assisted Position Mooring Systems for Ships”, *Proceedings of the 4th IFAC Conference on Manoeuvring and Control of Marine Craft*, Brijuni, Croatia, 1997.
- [48] O. M. Aamo and T. I. Fossen, “Finite Element Modeling of Mooring Lines,” *Mathematics and Computers in Simulation*, vol. 53, pp. 415-422, 2000.
- [49] O. M. Aamo and T. I. Fossen, “Finite Element Modelling of Moored Vessels,” *Journal of Mathematical and Computer Modelling of Dynamical Systems*, vol. 7, no. 1, pp. 47-75, 2001.
- [50] P. I. B. Berntsen, O. M. Aamo, B. J. Leira, “Ensuring Mooring Line Integrity by Dynamic Positioning: Controller Design and Experimental tests,” *Automatica*, vol. 45, no. 5, pp. 1285-1290, 2009.
- [51] D.T. Nguyen, A.J. Sørensen, “Switching Control for Thruster-assisted Position Mooring,” *Control Engineering Practice*, vol. 17, no. 9, pp. 985-994, 2009.
- [52] D.H. Nguyen, D.T. Nguyen, S.T. Quek, A.J. Sørensen, “Control of Marine Riser end Angles by Position Mooring,” *Control Engineering Practice*, vol. 18, no. 9, pp. 1013-1021, 2010.
- [53] K. Nai, W. Forsythe and R. M. Goodall, “Vibration Reduction Techniques for High Speed Passenger Elevators”, *Proceedings of the Third IEEE Conference on Control Applications*, Glasgow, vol. 2, pp. 965-970, 1994.
- [54] S. Ouchi, K. Z. Liu, S. Sato and T. Mita, “Mine Train Control System by H_∞ Control”, *Transactions of the Society of Instrument and Control Engineers*, vol. 34 , no. 3, pp. 225-231, 1998.

- [55] J. P. Strand, A. J. Sørensen and T. I. Fossen, “Design of Automatic Thruster Assisted Position Mooring Systems for Ships”, *Modeling, Identification and Control*, vol. 19, no. 2, pp. 61-75, 1998.
- [56] J. J. Gorman, K. W. Jablokow, and D. J. Cannon, “The Cable Array Robot: Theory and Experiment,” *Proceedings of IEEE International Conference on Robotics and Automation*, pp. 2804–2810, 2001.
- [57] E. Imanishi, T. Nanjo and T. Kobayashi, “Dynamic Simulation of Wire Rope with Contact”, *Journal of Mechanical Science and Technology*, vol. 23, no.4, pp. 1083-1088, 2009.
- [58] A. Cherubinia, A. Papinia, R. Vertechyb and M. Fontana, “Airborne Wind Energy Systems: A review of The Technologies”, *Renewable and Sustainable Energy Reviews*, vol. 51, pp. 1461-1476, 2015.
- [59] S. R. Oh and S. K. Agrawal, “Generation of Feasible Set Points and Control of a Cable Robot,” *IEEE Transactions on Robotics*, vol. 22, no. 3, pp. 551–558, 2006.
- [60] D. Lau, D. Oetomo, and S. K. Halgamuge, “Generalized Modeling of Multilink Cable-driven Manipulators with Arbitrary Routing using The Cable Routing Matrix”, *Transactions on Robotics*, vol. 29, no. 5, pp. 1102–1113, 2013.
- [61] M. Milutinovic, N. Kranjcevic and J. Deur, “Multi-mass Dynamic Model of a Variable-length Tether used in a High Altitude Wind Energy System”, *Energy Conversion and Management*, vol. 87, 1141:1150, 2014.
- [62] H. Takeuchi, K. Liu and S. Ouchi, “Velocity Control of a Mine Truck System using Rationally Scaled H_∞ Control”, *Proceedings of the 35th IEEE Conference on Decision and Control*, pp. 767-772, 1996.

- [63] J. K. Kang and S. K. Sul, "Vibration Control of Elevator Using Estimated Car Acceleration Feedback Compensation", *IEEE Transactions on Industrial Electronics*, vol. 47, no. 1, pp. 91-99, 2000.
- [64] S. M. Moon, J. Huh, D. Hong, S. Lee and C.S. Han, "Vertical Motion Control of Building Facade Maintenance Robot with Built-in Guide Rail," *Robotics and Computer-Integrated Manufacturing*, pp. 11-20, 2015.
- [65] K. Ogata, *Modern Control Engineering*, 4th ed., Prentice Hall, Upper Saddle River, NJ, 2002.
- [66] W. S. Levine, *The Control Handbook*, Vol. 1, CRC Press, Boca Raton, FL, 1996.
- [67] D.W. Gu, P.H. Petkov, M.M. Konstantinov, *Robust Control Design with MATLAB*, Springer-Verlag, London, 2013.
- [68] G. Balas, R. Chiang, A. Packard, M. Safonov, *Robust Control Toolbox User's Guide*, The Mathworks, Natick, 2012.
- [69] T. I. Fossen, *Marine Control System Guidance, Navigation, Rigs and Underwater Vehicle*, Trondheim, Norway: Marine Cybernetics, 2002.
- [70] M. S. Triantafyllow, "Cable Mechanics with Marine Application," lecture notes, Department of Ocean Engineering, Massachusetts Institute of Technology, Cambridge, MA 02139, USA, May 1990.
- [71] H. Kawai, Y. B. Kim and Y. Choi, "Measurement of a Container Crane Spreader under Bad Weather Conditions by Image Restoration," *IEEE Transactions on Instrumentation and Measurement*, vol. 61, no. 1, pp. 35-42, Jan. 2012.

Publication and Conference

Published Journal

- [1] **Anh-Minh D. Tran**, Sang-Won Ji and Young-Bok Kim, “A Ship Berthing System Design by Cooperating with Tugboats and Dampers,” *Journal of Drive and Control*, Vol. 11, No.3, pp. 7-13, 2014. **KOREA**, ISSN 2234-8328 (Print), / ISSN 2287-6146 (Online)
- [2] **Anh-Minh D. Tran**, Jung-In Yoon and Young-Bok Kim, “Motion Control System Design for a Barge Type Vessel Moored by Ropes,” *AETA 2015: Recent Advances in Electrical Engineering and Related Sciences, Lecture Notes in Electrical Engineering 371*, pp. 389-397, 2015. **SCOPUS**, ISBN 978-3-319-27245-0 (Print), / ISBN 978-3-319-27247-4 (Online)
- [3] **Anh-Minh D. Tran** and Young-Bok Kim, “Dynamics Identification and Robust Control Performance Evaluation of Towing Rope under Rope Length Variation,” *Journal of the Korea Society for Power System Engineering*, Vol. 20, No.2, pp. 58-65, 2014. **KOREA**, ISSN 1226-7813 (Print), / ISSN 2384-1354 (Online)
- [4] **Anh-Minh D. Tran**, Suk-Ho Jung, Jung-In Yoon and Young-Bok Kim, “Vessel motion control using rope tension control strategy,” *International Journal of Control, Automation and Systems*, Vol. 14, No. 4, pp. 915-923, 2016. Accepted for publication. DOI: 10.1007/s12555-015-0046-7. **SCIE**, ISSN 1598-6446 (Print), / ISSN 2005-4092 (Online)

Accepted Journal

- [5] **Anh-Minh D. Tran**, Jung-In Yoon and Young-Bok Kim, “ μ -Synthesis Robust Control on Tension Adjustment of Towing Rope System,” *Lecture Notes in Electrical Engineering series (Springer)*, **SCOPUS**, **ISI Proceedings**, (Accepted and to be published by Springer), Series ISSN 1876-1100.



International Conferences

- [1] **Anh Minh D. Tran**, Sukho Jung, Jiseong Jang, Jungin Yun, Changhyo Son, Kwanghwan Choi and Youngbok Kim, “A Ship Berthing Technology Assisted by Tugboats and Portable Dampers,” *Proceedings of 2014 International Symposium on Smart Sensing and Actuator System (ISSS’14)*, Busan, Korea, pp. 31-36, 2014.
- [2] **Anh Minh D. Tran**, Sukho Jung, Jiseong Jang, Jungin Yun, Changhyo Son, Kwanghwan Choi and Youngbok Kim, “A Study on Positioning Mooring System Design for Barge Ship,” *Proceedings of 2014 International Symposium on Smart Sensing and Actuator System (ISSS’14)*, Busan, Korea, pp. 39-44, 2014.
- [3] **Anh-Minh D. Tran**, Chang-Hyo Son, Jung-In Yun, Kwang-Hwan Choi, Suk-Ho Jung and Young-Bok Kim, “A study on floating unit motion control strategy,” *Control, Automation and Systems (ICCAS), 2015 15th International Conference on*, Busan, Korea, pp. 752-757, 2015.
- [4] **Anh-Minh D. Tran** and Young-Bok Kim, “A Study on Position Mooring System Design,” *Proceedings of 2015 International Symposium on Smart Sensing and Actuator System (ISSS’15)*, Hakone-Hachioji, Japan, pp. 68-73, 2015.
- [5] **Anh-Minh D. Tran**, Kazuhiro Watanabe, Yong-Woon Choi, Young-Bok Kim, “A Study on Position Mooring System for Barge Vessel,” *The 2015 International Symposium on Advanced Engineering (ISAE 2015)*, Busan, Korea, 2015.